

# Analysis of Rainfall Trends and Variability in Eastern Himalaya: Evidence from Sikkim

**Jyotirmayee Sarkar <sup>1</sup>, Yash Nayan <sup>2</sup> and Amrita Dwivedi <sup>1,\*</sup>**

<sup>1</sup> Department of Humanistic Studies, Indian Institute of Technology (BHU), Varanasi 221 005, Uttar Pradesh, India; [jyotirmayeesarkar.rs.hss23@itbhu.ac.in](mailto:jyotirmayeesarkar.rs.hss23@itbhu.ac.in); <https://orcid.org/0009-0004-7917-9548>

<sup>2</sup> Department of Civil Engineering, Indian Institute of Technology (BHU), Varanasi 221 005, Uttar Pradesh, India; [yashnayan8814@gmail.com](mailto:yashnayan8814@gmail.com); <https://orcid.org/0009-0007-9604-978X>

\* Corresponding Author: [amrita.hss@itbhu.ac.in](mailto:amrita.hss@itbhu.ac.in); <https://orcid.org/0000-0002-4950-2883>

**Abstract:** Since last century, Sikkim has witnessed substantial climatic fluctuations that can affect the local water availability, agricultural productivity, and livelihood security. Despite this growing concern, a limited study incorporated century-long datasets to explore the underlying climatic pattern of the state and often focuses only on trend analysis without applying a diverse set of statistical and spatial techniques. Hence, a comprehensive analysis has been employed to explore the long-term trend and variability of Sikkim's yearly and seasonal precipitation patterns from 1923 to 2023. Several statistical matrices have been applied viz. Coefficient of Variation (CV), Analysis of Variance (ANOVA) and Tukey's Honest Significant Difference (HSD) Test to analyze the intra-seasonal and inter-seasonal rainfall variability, Standardized Precipitation Index (SPI) has been used to find out wet and dry years, Precipitation Concentration Index (PCI) shows annual and seasonal rainfall distribution, Simple Moving Average method has been applied to detect long-term trend, Inverse Distance Weighted interpolation technique visualizes the spatial rainfall variation in the state. This research offers new insights into the precipitation behavior and shifting rainfall dynamics such as summer rainfall demonstrates the most significant inter-cluster difference, wet and dry events are significantly increasing in summer season, the highest variability in precipitation distribution can be observed in monsoon rain, the summer and winter rainfall is increasing, where monsoon rainfall is decreasing significantly over the region, monsoon rainfall shows significant increasing trend in Gyalshing and Mangan, where summer and winter rain is increasing at Gyalshing and Mangan. These findings can help in regional adaptation strategies, water resource management, agricultural planning, and minimize climate-related livelihood vulnerabilities, as most of the farmers of this state rely on rainfall for their irrigation purposes.

**Keywords:** Sikkim Himalaya; Rainfall Variability; Rainfall Trend; SPI; PCI; ANOVA; Agricultural Vulnerability

## 1. Introduction

The concept “climate Change” hardly requires any further validation in the present scenario (Gunawat et al., 2022; Sharma et al., 2022; Carbonary et al., 2025). It is a long-term global phenomenon which involves the complex interactions of environment, socioeconomic, and political processes. Though climate change and variability are natural processes, these are severely intensifying due to anthropogenic causes since the 20th and 21st centuries (IPCC, 2023; Gao, 2021; Tapia-Brito & Riffat, 2025). Little changes in climatic elements, e.g., temperature, rainfall, etc. can significantly affect agricultural productivity, which in turn escalates poverty and the overall well-being of people (Lee et al., 2016; Ghosh & Ghosal, 2021; CUCE, 2025). The varying rainfall amount and intensity are among the most significant climatic elements contributing to determining stream flow pattern, runoff, groundwater reserves, soil moisture, etc. Already, global warming-induced changes in rainfall can be witnessed in various regions, which can significantly impact global water demand and agricultural productivity (Ojo & Ilunga, 2017; Kakkar et al., 2022). The changing rainfall behavior can trigger the incidents of floods and droughts.



According to the IPCC report (2007), the freshwater availability will be reduced by the mid twenty-first century, and which is projected to be up to 10-30%. In the Indian context, the agricultural system primarily depends on monsoonal rainfall. Therefore, the changing precipitation pattern can broadly impact water resource planning and management (Chakraborty et al., 2013).

Mountains are most fragile to varying climatic behavior and are already experiencing temperature rise, especially at higher altitudes (Schröder et al., 2024; Xu et al., 2009). The vulnerable of mountain people is very high due to the characteristics of marginality, fragility, remoteness, poor accessibility to infrastructure and market facilities, and, primary reliance upon the agricultural economy, and natural resources (Macchi et al., 2015; Bhatta et al., 2015; Gerlitz et al., 2017; Chettri et al., 2018). Sikkim is also a part of these mountain systems and stands out as a critical case for understanding climatic variability due to mountain terrain, monsoon dependency, and predominantly agrarian economy. This state mainly receives rainfall from the southwest monsoon. Besides, it gets very little rain from western disturbances and north-east monsoon (Kumar et al., 2020). Altering precipitation impacts river runoff, groundwater recharge, soil moisture, and agricultural productivity in Sikkim Himalayas (Sharma & Shreshtha, 2016). Most farmers in Sikkim practice traditional farming methods depending on local raw materials and indigenous techniques, making it more sensitive to climatic changes and variability (Mishra et al., 2020; Upadhyay et al., 2024). According to SAPCC (2011), the rainfall projection 2030 shows a 12 mm decline in winter rainfall and an overall decrease in precipitation by 30%. The short heavy rainfall increases surface runoff, significantly affecting groundwater recharge (Basu et al., 2021).

Regardless of rising apprehension of climate variability in Eastern Himalayas, a few studies conducted centennial analysis of precipitation patterns of Sikkim. Additionally, these existing studies heavily rely on trend detection without implementing broader statistical and spatial analysis to investigate long-term rainfall patterns. As a result, there remains a significant gap in capturing the long-term dynamics in precipitation across the state. For instance, Kakkar et al. (2022) analyzed precipitation patterns of Sikkim over 115 years but only focused on trend analysis and NDVI measurements to find moisture availability. Another research by Sharma et al. (2025) analyzed 123 years of rainfall in Gangtok and Itanagar by employing trend and anomaly analysis but did not apply ANOVA, SPI, PCI, or spatial mapping techniques. None of the studies link findings to sectorial or livelihood considerations. Hence, research on regional climatic patterns and their influence on economy and social setup are crucial, as very few studies are available on this region. This study aims to address these gaps by considering a hundred-year rainfall data with a range of statistical methods and spatial investigation of precipitation behavior across Sikkim. Unlike previous work limited in methodological scopes and lacking clear connections to livelihood impacts, this study applies SPI, PCI, and IDW to model rainfall variability across all seasons and districts of Sikkim, offering a spatial-temporal lens associated to agricultural exposure exacerbating livelihood vulnerability.

## 2. Materials and Methods

This research aimed to evaluate spatial and temporal rainfall behavior of Sikkim over a period hundred years. The study is oriented towards the following objectives:

1. To detect long-term trends and visualize spatial variations
2. To identify inter-seasonal and intra-seasonal rainfall variability
3. To detect extreme events (wet and dry periods) and changes in precipitation concentration

To ensure a comprehensive coverage of precipitation behavior, each method has been selected to address specific dimensions, for example- descriptive (CV) and inferential statistics (ANOVA, Tukey's HSD Test) used to detect seasonal rainfall variability; SPI and PCI applied to identify extreme events and seasonal rainfall distribution, respectively; and IDW interpolation technique applied to visualize spatial rainfall pattern and trend.

### 2.1. Data Source

Gridded precipitation data of the five weather stations in Sikkim have been collected from the India Meteorological Department (IMD) with a grid cell size of  $0.25 \times 0.25$ . As per the World Meteorological Organization (WMO) and the National Oceanic and Atmospheric Administration (NOAA), 30 years of the average atmospheric condition is considered to define it as climate (Getahun et al., 2016). Hence, to identify a broader pattern of changes and variability of climate, a total of 100 years of rainfall has been taken. The details of weather stations are given in Table 1.

**Table 1.** Details of the Weather Stations of Sikkim.

Sl. No.	Name of the Weather Stations	Latitude	Longitude	Elevation (m)	District
1.	Mazitar	27.1833° E	88.5333° E	300	East Sikkim
2.	Mangan	27.5167° N	88.5225° E	1000	North Sikkim
3.	Namthang	27.1667° N	88.3640° E	800	South Sikkim
4.	Gyalshing	27.2750° N	88.2710° E	1200	West Sikkim
5.	Tadong	27.3389° N	88.6122° E	1400	East Sikkim

(Source: IMD)

## 2.2. Coefficient of Variation (CV)

CV is a prevalent method to identify variability in a dataset. It represents how much a set of numbers varies relative to its mean. This method removes units by dividing the standard deviation by the mean, which makes the dataset comparable with different units or scales (Abdi, 2010). CV has been applied here because it standardizes the variability, and it becomes easy to compare across different seasons and time periods. A higher CV indicates higher rainfall variability and vice versa. Some limitations prevail in the method, such as CV is highly sensitive to mean values. A low mean value, even a slight standard deviation, can result in a very high variation (Livers, J.J., 1942). The coefficient of variation is calculated using the following equation:

$$CV = \frac{\sigma}{\mu} \times 100 \quad (1)$$

Here, CV represents the Coefficient of Variation  
 $\sigma$  means Standard Deviation, and  $\mu$  signifies the mean of rainfall

## 2.3. One Way Analysis of Variance (ANOVA)

ANOVA is a widely used parametric statistical technique to find variation between two or more groups of observations by comparing their mean values (Umar et al., 2019; Larson, M.G., 2008). This method has been applied to test whether the seasonal rainfall varies significantly between groups. ANOVA is based on mathematical linear regression and general linear models that can quantify the relationship between response and explanatory variables (Sawyer, S.F. 2009). The sources of variation are recognized by comparing the between and within-group variability. The F value is measured and compared with the F critical ratio to establish the acceptance or rejection of the hypothesis (Agada, 2018). ANOVA, though powerful for variability testing, has some limitations. It assumes that data in all groups are normally distributed and have equal variance. Further, it only tells that differences exist in mean values but cannot identify which groups are different from others (Buckland & Ravenscroft, 1990). In this study, only one independent variable is taken for analysis, which is rainfall. Since ANOVA is suitable for detecting statistically significant mean differences across groups, it is applied to identify systematic variations in rainfall between and within clusters over time.

## 2.4. Tukey's HSD Test

The result of the Analysis of Variance only exhibits a significant difference between groups, which suggests that at least one group differs from another group. However, these findings do not show the pattern of differences between means and which group differs from which one. To analyze these patterns of differences, Tukey's Honest Significant Difference Test has been applied in this study. It is a pairwise comparison technique between the means of two groups using a statistical distribution called q distribution. The q value should be greater than the q critical to a significant difference between the two groups (Abdi & Williams, 2010). Like ANOVA, this method works on homogenous data and is designed for equal variance for each group (Agbangba et al., 2024). The Tukey's HSD can be computed with the following equation:

$$|Ma^+ - Ma'^+| > HSD = q \sqrt{\frac{MSE}{2} \times \left( \frac{1}{S_a} + \frac{1}{S_{a'}} \right)} \quad (2)$$

Here,  $|Ma^+ - Ma'^+|$  represents the comparison between two groups

HSD is Honest Significant Difference

q signifies Studentized Range Statistic, which is obtained from Tukey's q table

MSE defines Mean Squared Error, which can be calculated from ANOVA

$S_a$  and  $S_{a'}$  are the sizes of two groups being compared

## 2.5. Standardized Precipitation Index (SPI)

Standardized Precipitation Index is a statistical method to investigate the intensity and duration of drought events at a place (Livada & Assimakopoulos, 2007). SPI is selected to detect and quantify extreme wet and dry periods over the centennial time frame in Sikkim. This method transforms rainfall data into a normalized index, which is helpful for comparing across regions and time scales. It is crucial for drought and flood risk management in a region. The rainfall data was first fitted into a gamma probability distribution to calculate SPI, which is applied for modeling nonnegative precipitation values. As precipitation data is always nonnegative and follows a skewed distribution rather than normal distribution, the gamma probability density function (PDF) is applied to transform the rainfall data into a normal distribution (Raziei, 2021; Karavitis et al., 2011). Though widely used, SPI has practical limitations to be applied in mountainous region and when deal with sparse datasets from a few weather stations. Mountains often record zero rainfall in drier months and due to orographic nature of rainfall, it often produces skewed distribution. SPI is sensitive to the distribution of rainfall data. Sparse weather stations further limit the representativeness of SPI values, which may fail to capture localized variability. It assumes that precipitation follows gamma distribution, which may not always provide a perfect fit, particularly in regions where rainfall is highly skewed or zero rainfall events are widespread (Sienz et al., 2012). As our dataset for seasonal monthly mean does not contain any zero rainfall event, the issue of handling of zero precipitation is not encountered. Moreover, gamma distribution provides an appropriate fit for the skewed rainfall, ensuring the results are not distorted. Besides, SPI often underestimates the intensity of dryness or wetness when rainfall is very low or very high (Kumar et al., 2009). Also SPI considers equal threshold value for both humid and arid regions. A particular SPI value can mean mild dryness in humid regions but a severe drought in arid zones. Yet SPI labels both in the same category. Hence fixed threshold method may not fully capture the real hydrological impacts (Cheval, S. 2015). As the analysis is confined to a single region without any comparison between humid and dry climates, the fixed threshold value can be reliable in this context. The PDF of the gamma distribution is given by:

$$g(x, \alpha, \beta) = \frac{1}{\beta^\alpha \cdot \Gamma(\alpha)} x^{\alpha-1} \cdot e^{-x/\beta} \quad (3)$$

Here,  $\alpha$  is the shape parameter,  $\beta$  is the scale parameter, and  $\Gamma(\alpha)$  is the gamma function. The shape and scale parameters were estimated using maximum likelihood estimation. The cumulative probability function ( $G(x)$ ) was then obtained by integrating the gamma distribution. The cumulative distribution is calculated by:

$$G(x) = \int_0^x g(t) dt \quad (4)$$

Since gamma distribution is undefined for zero precipitation, a mixed distribution approach was applied, incorporating the probability of zero precipitation events. The computed cumulative probabilities were then transformed into a standard normal distribution using the inverse normal function, ensuring that SPI values have a mean of 0 and a standard deviation of 1. The inverse normal function is given below:

$$SPI = \Phi^{-1}(G(x)) \quad (5)$$

Here,  $\Phi^{-1}$  represents the inverse cumulative distribution function of the standard normal distribution. After this calculation, the SPI values are classified in nine classes (Table 2) as per Hänsel et al.(2016):

**Table 2.** Standardized Precipitation Index Classes.

SPI	Class Description
$\geq 2$	Extremely Wet
1.50 to 1.99	Very Wet
1.00 to 1.49	Moderately Wet
0.50 to 0.99	Slightly Wet
-0.49 to 0.49	Near Normal
-0.99 to -0.50	Slightly Dry
-1.49 to -1.00	Moderately Dry
-1.99 to -1.50	Very Dry
$\leq -2$	Extremely Dry

(Source: Hänsel et al., 2016)

## 2.6. Precipitation Concentration Index (PCI)

The Precipitation Concentration Index is a method that measures the monthly, seasonal, and annual rainfall distribution in a region (Belay et al., 2021). This statistical technique helps to identify if the rainfall is concentrated or evenly distributed over some time. The precipitation concentration is important to identify as it helps in water resource planning and crop productivity, especially in a rainfed-dependent state like Sikkim. The higher PCI values indicate that rainfall is concentrated in fewer months. On the contrary, smaller values show the uniform distribution of precipitation. PCI computation helps identify the drought and flooding risks (Michaels et al., 1998). Though valuable to identify precipitation distribution, PCI is sensitive to outliers. One or two months of abnormal rainfall can skew the index or overstate variability. Monthly mean rainfall dataset used in this study does not include any anomalous extreme that can misrepresent the outcome. Further, the standard threshold values of PCI were developed by for Mediterranean climates, which may not be fully appropriate for the Himalayan context (Oliver, 1980). As there is no specific PCI statistic particularly designed for mountainous context, the conventional PCI is applied to find out the general distribution pattern of rainfall. PCI values are classified in four categories and described in Table 3. PCI can be calculated using the following formulas:

$$\text{PCI}_{\text{annual}} = \frac{\sum_{i=1}^{12} p_i^2}{(\sum_{i=1}^{12} p_i)^2} \times 100 \quad (6)$$

$$\text{PCI}_{\text{seasonal}} = \frac{\sum_{i=1}^3 p_i^2}{(\sum_{i=1}^3 p_i)^2} \times 25 \quad (7)$$

Here,  $P_i$  is the monthly precipitation for month  $i$ .

**Table 3.** Precipitation Concentration Index Classes.

PCI Values	Class Description
<10	Uniform Rainfall Concentration
11-15	Moderate Rainfall Concentration
16-20	Irregular Rainfall Concentration
>20	Extremely Irregular Rainfall Concentration

(Source: Birara et al., 2018)

## 2.7. Moving Average

In a time series analysis, moving average is a widely applied technique to find trends in a dataset. This method has been applied to smooth the short-term fluctuations in the rainfall dataset and to highlight long-term trends, which provides easier visualization of gradual climatic shifts over a century-long time period. (Hansun, S. 2013). In our present study, the simple moving average method has been applied which assigns equal weight to every point. SMA is excellent for smoothing the short-term fluctuations in the data and visualizes the changes in rainfall pattern. But simple moving average method assigns equal weights to all the values, which can underrepresent the recent fluctuations (Johnstone et al., 1999). SMA is calculated by using the following equation:

$$\text{SMA}_t = \frac{1}{N} \sum_{i=0}^{N-1} X_{t-i} \quad (8)$$

Here, SMA $_t$  means Simple Moving Average

N is the number of period in the moving average window

$X_{t-i}$  is the observed value at time  $t-i$

i is the index of summation, starting from 0 up to N-1

## 2.8. Interpolation

Interpolation is a widely used method that estimates the values of unknown points depending on the known values of discrete data points. This study applied the interpolation technique to estimate the seasonal rainfall distribution and trend of the unknown places based on the five weather stations in Sikkim. Here the Inverse Distance Weighted (IDW) technique has been applied by using ArcGIS 10.5. This is the most common local interpolation method. IDW has been chosen due to its simplicity and suitability for a few known points. In Sikkim's complex terrain, IDW provides a locally weighted estimation that prioritizes nearby observations, making it appropriate for capturing regional rainfall patterns across limited stations. The basic concept behind this method is that the estimated value of a point is influenced more by the nearby known points than the points which are further away (Chang, K.T. 2016). Although this method is helpful for a few known data points, it has some limitations. The

limitations are particularly relevant for mountainous regions like Sikkim where rainfall is strongly controlled by topography and sparse data from fewer weather stations may reduce the accuracy of interpolation as IDW interpolation assumes spatial homogeneity and does not account for topographic effects (Li & Heap, 2014). This method is based on inverse distance weighting but does not consider the spatial autocorrelation. The result of this method is sensitive to outliers and influenced by the way observations have been sampled. The datasets clustering can cause estimation bias (Gentile et al., 2012). The value of unknown location  $Z_x$  is estimated as:

$$Z_x = \frac{\sum_{i=1}^n w_i z_i}{\sum_{i=1}^n w_i}$$

The weights  $W_i$  are calculated as:

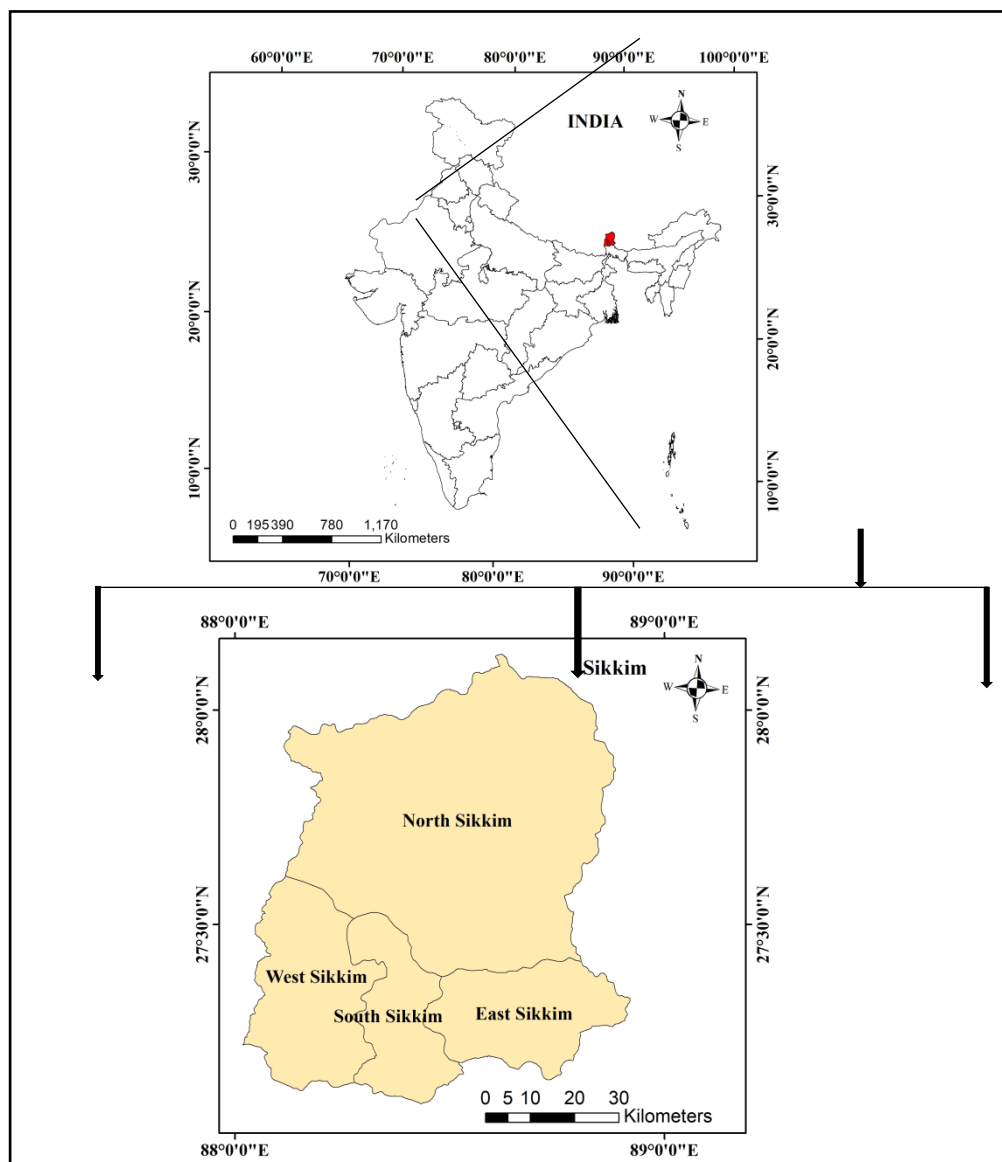
$$W_i = \frac{1}{d_i^p} \quad (9)$$

where  $Z_x$  is the unknown data point

$W_i$  is the weight assigned to the  $i^{\text{th}}$  sample point, calculated as the inverse of distance raised to a power  $p$

$Z_i$  is the known value of the  $i^{\text{th}}$  sample point

$d_i^p$  is the distance between the unknown point and the  $i^{\text{th}}$  sample point



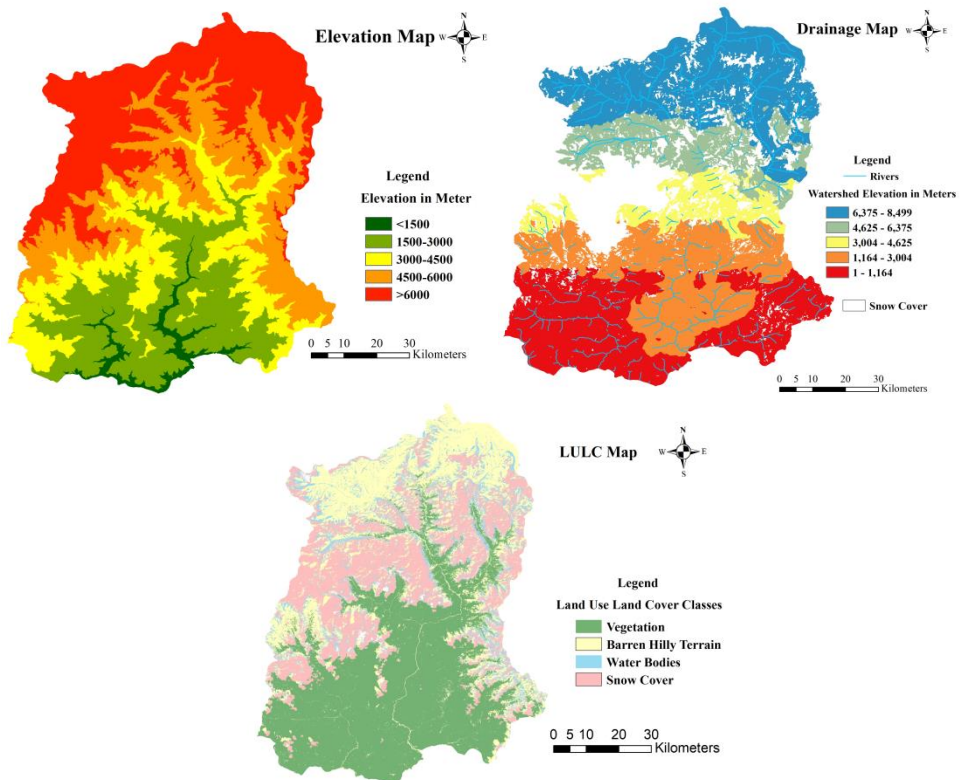


**Figure 1.** Location Map of Study Area.

### 2.9. Study Area

Sikkim is a northeastern state and also the second smallest state in the region. It shares its border with three countries: Nepal in the west, Bhutan in the east, and Tibet in the north. West Bengal is situated in the south. The state extends between  $27^{\circ}04'$  north and  $28^{\circ}07'$  north latitude and  $88^{\circ}00'$  east and  $88^{\circ}55'$  east longitude. Teesta, Rangit, Rangpo, and Lachen are the major rivers that flow through this state. It is a mountainous state where altitude varies from 300 meters to 8586 meters. Kangchenjunga, the third-highest mountain peak in the world and second-highest mountain peak in India, situated in this state. This state is also home to some of the largest glaciers of the Eastern Himalayas, which are Zemu, Rathong, Lohnak, etc. The climate of Sikkim varies from tropical to tundra type. The temperature fluctuates from below  $0^{\circ}$  Celsius in winter to  $28^{\circ}$  Celsius in summer. Besides, the yearly precipitation ranges from 2700 millimeters to 3200 millimeters. The state consists of four districts viz. North, South, East, and West Sikkim (Sikkim FSI, 2019). Total population of this state is 610577 (Government of Sikkim, 2011). The Majority of Sikkim's population belongs to the rural population, which comprises 75.03% of the population. The population density of this state is 86 persons per square kilometer (Sikkim Statistics, 2013). Among these, 75% of the rural population, 80% people is dependent on agricultural activities and livestock farming (Lama, 2001). The location map of the study area is given in Figure 1.

The following section of this paper presents the findings derived from the statistical and spatial analysis. It begins with a general description of seasonal and annual rainfall distribution, followed by analysis of variance, standardized precipitation, precipitation concentration, trend detection, and spatial analysis. These findings will uncover the long-term trends and variability critical for understanding shifting climatic behavior in Sikkim.

## 3. Results and Findings

This section portrays the key findings of this research based on temporal and spatial analysis of precipitation patterns of Sikkim. Firstly, it shows the seasonal distribution of precipitation, followed by statistical and spatial analyses. The outcomes are analyzed to understand rainfall variability, annual and seasonal rainfall trends, rainfall distribution, occurrences of extreme events, and spatial patterns across the state. These findings provide a crucial insight into potential climatic shifts in the state.

### 3.1. Descriptive Statistics of Rainfall

The rainfall data provided an insight into rainfall distribution over Sikkim. The mean seasonal precipitation of Summer, Monsoon, Post Monsoon, and Winter over the years is 465.51, 1745.998, 547.296, and 56.93667 respectively. The analysis of rainfall distribution of different seasons (Figure 2) exhibits that the monsoon shares the highest amount of precipitation, which is 62%. 19% is contributed by the post monsoon, which makes it the second rainiest season. While summer and winter contribute up to 17% and 2% respectively.

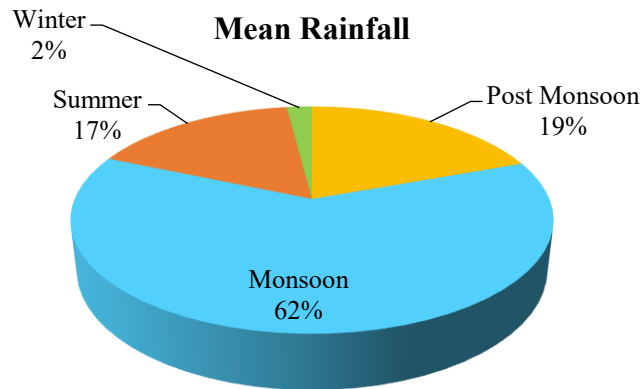


**Figure 2.** Seasonal Mean Annual Rainfall Distribution in Sikkim from 1923-2023.

### 3.2. Coefficient of Variation

Like the mean rainfall, the variability is also high within the seasons. The graph (Figure 3) illustrates the coefficient of variation of the four seasons' precipitation from 1924 to 2023. The highest variability could be observed in the winter rainfall with several sharp peaks and significant declines. A variability of about 121% can be noticed between 1964 and 1968; on the other hand, only up to 16% could be observed between 2019 and 2023. This pattern illustrates episodic heavy rainfall incidents rather than a consistent seasonal pattern. In contrast, the monsoon exhibits the lowest percentage of variation with minor peaks and falls, suggesting a steady monsoonal influence. The highest variation rate is 25%, which occurred between the period of 1994 and 1998, and the lowest variability is only 3% from 1929-1933. Besides, a moderate level of variability could be seen in post monsoon and summer rainfall, with no extreme fluctuations. In post monsoon rainfall, the highest variability could be noticed between 1964 and 1968, whereas the lowest variation of 8% occurred between 2009 and 2013. In contrast, the summer season shows the highest percentage of variability of 37% in 1959-1963 and the lowest variation between 2004 and 2008 with 6% of the variability. The above discussion indicates that while monsoons remain more or less consistent over the periods, the winter rainfall becomes more erratic. Summer and post monsoon seasons show moderate variability. These variations could be related to shifts in atmospheric circulation, weather patterns, and regional hydrological changes.

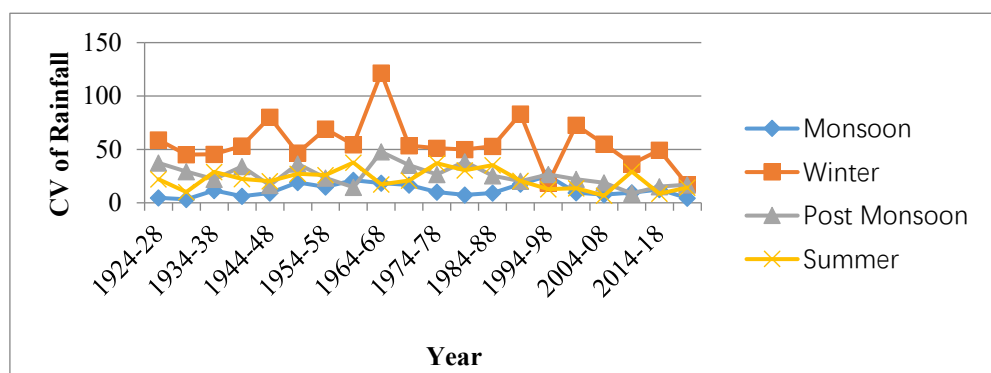
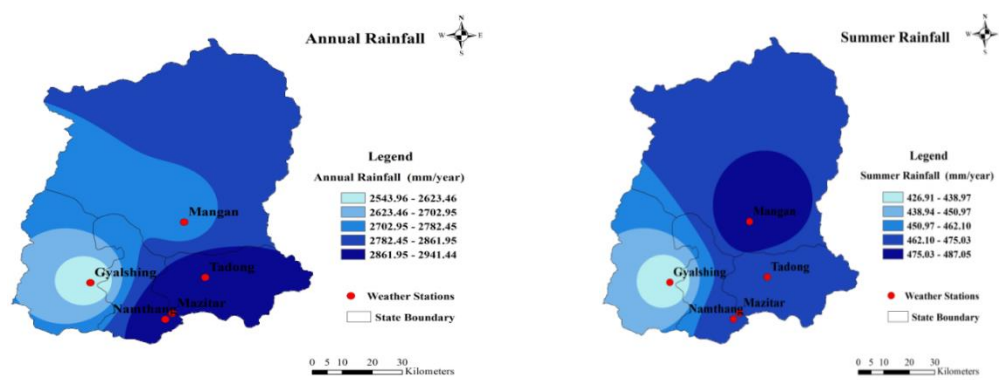


**Figure 3.** Seasonal Rainfall Variability of 20 clusters from 1923-2023.

### 3.3. Rainfall Pattern

Sikkim's spatial rainfall maps (Figure 4) reveal distinct yearly and seasonally precipitation distribution. The annual rainfall map shows that highest rainfall distribution is concentrated over the southeastern part, followed by the northeastern region, with values ranging from 2782.45 to 2941.44 mm per year. Conversely, the lowest distribution can be seen in the southwestern part, with an average rainfall of 2543.96 to 2702.95 mm per year.

A similar pattern of rainfall distribution can be observed in the monsoon and post monsoon season, with the highest amount concentrated over the southeastern and the northeastern parts of the state, with values ranging from 1734.34 to 1842.04 mm and 541.90 to 573.55 mm per year, respectively. Lowest rainfall amount is concentrated over the southwestern part, with average rainfall amount of 1572.79 to 1680.49 mm in the monsoon season and 494.43 to 526.08 mm per year in the post monsoon season. As monsoon and post monsoon seasons share the major yearly rainfall, these influence the annual rainfall distribution pattern. Besides, in the summer season, the principal precipitation amount is concentrated in the central part, and the second highest concentration is located in the significant portions of the northern, southern, and eastern parts of Sikkim, where the rainfall amount varies from 462.10 to 487.05 mm per year. Here also, the lowest rainfall occurs in the southwestern part. For winter months, the highest rainfall distribution can be noticed in the central part, with rainfall amounts varying from 64.15 to 73.70 mm per year, whereas the lowest share of rainfall can be seen in the southern and the southwestern parts with rainfall amounts of 49.83 to 59.38 mm per year. In the monsoon season, the southeastern and eastern part receives the highest amount of rainfall, and the reason behind this can be attributed to the path of the southwest monsoon wind. During monsoon, the moisture-carrying winds from the Bay of Bengal strike the southeastern and eastern slopes of Sikkim and bring down heavy amounts of rainfall over these regions. Similarly, these regions also receive a higher rainfall in post monsoon season. As the southwest monsoon wind retreats, the southeastern and eastern part of Sikkim continuously receives lingering moisture-laden rainfall. On the other hand, higher summer rainfall concentration in the central part can be attributed to the local orographic uplift of moisture-laden winds due to snowmelt moisture availability in this season. The southwest monsoon winds also start developing at this time, which supplies moisture to the northern, eastern, and southern regions of Sikkim, which lies in the path of southwest monsoon winds. The winter rainfall is also higher around the central part. The central part has a relatively lower elevation than the northern hilly terrain, so it receives lighter rain during snowfall. Besides, the southern and southwestern parts of Sikkim receive relatively lower precipitation compared to other parts of the state. The reason behind this phenomenon is the region's geographic location known as the rainshadow effect. The southern and southwestern part is located on the leeward side of the mountain ranges, which receive less moisture after rain on the windward side of the mountain range.



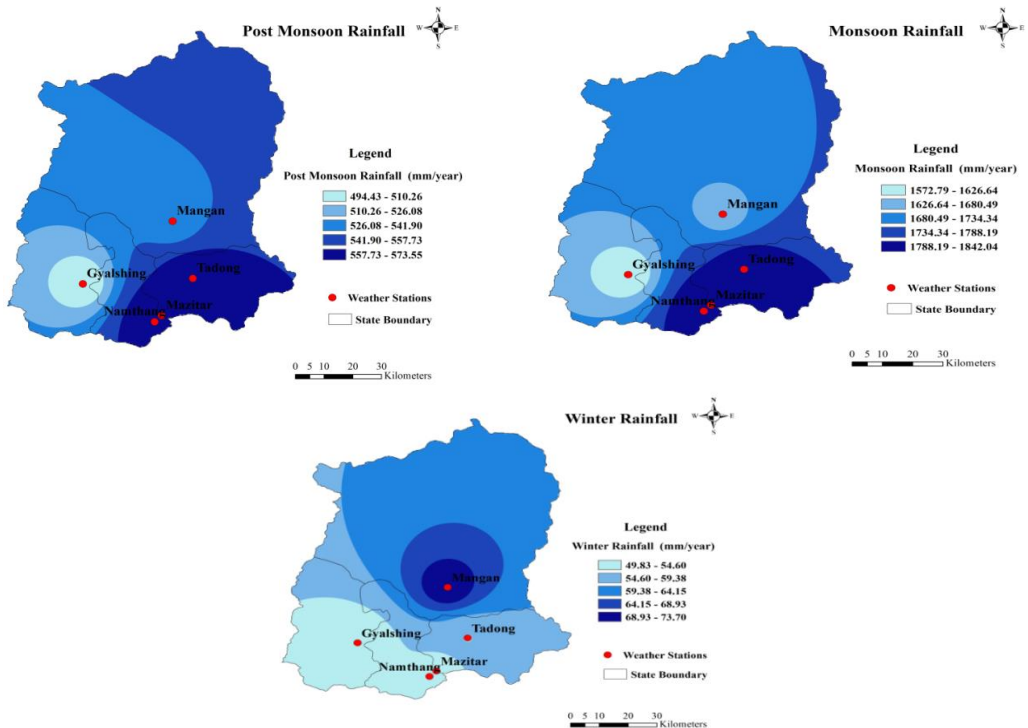


**Figure 4.** Annual and Seasonal Mean Rainfall Pattern across Sikkim from 1923-2023 based on IDW Interpolation Technique.

**Table 4.** Root Mean Square Error Analysis of Seasonal Mean Rainfall of Five Weather Stations.

Station	Summer			Monsoon			Post Monsoon			Winter			
	ns	AV	IV	RMS E	AV	IV	RM SE	AV	IV	RM SE	AV	IV	RM SE
Gyalshing	426.907	426.907	324	0.002	1572.79	1572.79	0.0	494.43	494.43	0.00	49.8	49.8	0.00
Mangan	487.059	487.055			1647.59	1647.62		530.530	530.530		73.7	73.7	
Majitar	471.202	470.205			1836.53	1836.55		570.570	570.570		53.7	53.7	
Namthang	471.202	471.201			1836.53	1836.52		592.592	589.59		163	163	
Tadong	471.202	471.203			1836.53	1836.53		570.570	570.570		53.7	53.7	
<b>Average</b>								592	592		163	168	

AV= Actual Values, IV= Interpolated Values, RMSE= Root Mean Square Error (Source: Compiled by Authors)

The Table 4 complements the spatial analysis by presenting the error analysis of IDW interpolation of seasonal mean rainfall across five weather stations. The table compares of actual values of rainfall of those five stations and interpolated values of IDW method for summer, monsoon, post monsoon and winter seasons. All the actual and interpolated values are nearly identical, indicating that applied interpolation method yielded highly accurate results. This statement is further supported by the root mean square error values, which are very small; for example, RMSE is 0.0023 for the summer season, 0.016 for the monsoon, 0.0027 for the post monsoon and 0.0016 for the winter season, which affirm the reliability of the interpolation method.

### 3.3 Analysis of Variance

The One way ANOVA was computed to find out the inter-seasonal variability of mean rainfall in 20 clusters (Table 5). Table 5 consists of five columns where the variables are the seasons, n means the number of observations, df refers to the degree of freedom, which is the number of independent values that can vary in an analysis, F represents the ratio between group variance and within-group variance,

and P value represents whether the difference is significant or not. The result shows significant differences in mean precipitation between seasons. Monsoon exhibits the highest mean, 1743 mm, whereas winter has the lowest mean, 58mm ([Table 5](#)).

**Table 5.** ANOVA for Inter-Seasonal Mean Rainfall.

Variables	n	Mean±SD	df	F	P Value (<0.05)
Monsoon	19	1743±30.26186	3	573.3179	0.000
Winter	19	57.78475±30.26186			
Summer	19	3339±30.26186			
Post Monsoon	19	549.5373±30.26186			

(Source: Compiled by Authors)

**Table 6.** Tukey's HSD Test for Inter-Seasonal Mean Rainfall.

Variables	Mean Difference	HSD ( $ M1-M2 >HSD$ )	Significance
Monsoon-Winter	1685.215247	219.6833569	Yes
Monsoon-Post Monsoon	1193.46274	219.6833569	Yes
Monsoon-Summer	1271.666069	219.6833569	Yes
Winter-Post Monsoon	491.7525076	219.6833569	Yes
Winter-Post Monsoon	413.5491781	219.6833569	Yes
Post Monsoon-Summer	78.20332947	219.6833569	No

(Source: Compiled by Authors)

As ANOVA only states the differences in seasonal rainfall, Tukey's HSD test has been applied further to explore which seasons differ significantly from each other ([Table 6](#)). Each season has been divided into 20 clusters with 5 years in each over hundred years and then the analysis has been done.

**Table 7.** ANOVA for Intra-Seasonal Mean Rainfall.

Variables	n	df	F	P Value (<0.05)	Significance
Monsoon	5	19	2.553686	0.0019359	Yes
Winter	5	19	2.449501	0.0029389	Yes
Post Monsoon	5	19	1.181091	0.2944569	No
Summer	5	19	7.700183	0.000	Yes

(Source: Compiled by Authors)

**Table 8.** Between and Within Cluster Variability across Seasons.

Seasons	Between Groups	Within Groups	F	P value	F Crit	Significance
Summer	2165150	1183922	7.700183	0.000	1.718	Yes
Monsoon	3420167.563	5639183.783	2.553686	0.001936	1.718	Yes
Post Monsoon	663206.7844	2364297.455	1.181091	0.294457	1.718	No
Winter	84494.59137	145240.4568	2.449501	0.002939	1.718	Yes

(Source: Compiled by Authors)

[Table 7](#) reveals the findings from the intra-seasonal ANOVA test indicating whether mean rainfall varied significantly within each season over time. All the seasons except post monsoon show significant differences, confirming intra-seasonal variability ([Table 7](#)). [Table 8](#) is a part of the ANOVA analysis, where it reflects the between and within-clusters variability of the three seasons, which helps to distinguish whether changes in rainfall are prominent across half decades or within short time intervals. For both monsoon and winter rainfall, the within-cluster variability is higher, about 5639183.783 and 145240.5, than the between-cluster variability, which is 3420167.563 and 84494.59, respectively. This indicates that the individual data are more varied from the mean of individual groups than the mean values between the groups, revealing that rainfall frequently varies within clusters. But in the context of the summer period, the situation is reversed as the between-group variability is higher, about 2165150, than within-group variability, which is 1183922, indicating clusters differ greatly.

### 3.4. Tukey's HSD

Further, Tukey's HSD test has been applied to identify which clusters differ significantly from others in seasonal rainfall ([Table 9, 10, & 11](#)). In the case of the monsoon season, a total of ten pairs of clusters

exhibit significant differences. On the other hand, winter shows seven pairs of clusters, which differ significantly. For the summer season, the highest number of different pairs could be identified, which is thirty-five. Hence, the difference between the five-year clusters is much higher in the summer season than in other periods.

**Table 9.** Tukey's HSD Test for Monsoon Rainfall.

Variables	Mean Difference	HSD( M1-M2 >HSD)	P Value (<0.05)
1929-33 to 1949-53	759.97772	615.4026152	0.0031190
1934-38 to 1949-53	663.176436	615.4026152	0.0214082
1944-48 to 1949-53	624.443676	615.4026152	0.0428695
1949-53 to 1959-63	907.114912	615.4026152	0.000113
1949-53 to 1969-73	617.572004	615.4026152	0.048233
1949-53 to 1989-93	823.866576	615.4026152	0.000775
1949-53 to 1999-03	793.31998	615.4026152	0.001524
1949-53 to 2004-08	773.329856	615.4026152	0.002348
1949-53 to 2009-13	770.808332	615.4026152	0.002478
1949-53 to 2014-18	808.48394	615.4026152	0.001092

(Source: Compiled by Authors)

**Table 10.** Tukey's HSD Test for Winter Rainfall.

Variables	Mean Difference	HSD( M1-M2 >HSD)	P Value (<0.05)
1924-28 to 1989-93	102.634548	98.7631689	0.03290
1944-48 to 1989-93	109.035056	98.7631689	0.01577
1959-63 to 1989-93	99.391564	98.7631689	0.04681
1964-68 to 1989-93	116.035952	98.7631689	0.00669
1969-73 to 1989-93	124.096372	98.7631689	0.00235
1974-78 to 1989-93	101.619192	98.7631689	0.03680
1989-93 to 2014-18	110.885904	98.7631689	0.01264

(Source: Compiled by Authors)

**Table 11.** Tukey's HSD Test for Summer Rainfall.

Variables	Mean Difference	HSD( M1-M2 >HSD)	P Value (<0.05)
1924-28 to 2014-18	444.371992	281.9764567	0.000
1924-28 to 2019-23	396.938288	281.9764567	0.000295
1929-33 to 2014-18	440.821716	281.9764567	0.000
1929-33 to 2019-23	393.388012	281.9764567	0.000352516
1934-38 to 2014-18	413.216712	281.9764567	0.000128269
1934-38 to 2019-23	365.783008	281.9764567	0.001366655
1939-43 to 2009-13	310.418512	281.9764567	0.016369054
1939-43 to 2014-18	477.245304	281.9764567	0.000
1939-43 to 2019-23	429.8116	281.9764567	0.000
1944-48 to 2009-13	296.462512	281.9764567	0.028773021
1944-48 to 2014-18	463.289304	281.9764567	0.000
1944-48 to 2019-23	415.8556	281.9764567	0.000111885
1949-53 to 2009-13	311.681064	281.9764567	0.015533149
1949-53 to 2014-18	478.507856	281.9764567	0.000
1949-53 to 2019-23	431.074152	281.9764567	0.000
1954-58 to 2009-13	363.983548	281.9764567	0.001489326
1954-58 to 2014-18	530.81034	281.9764567	0.000
1954-58 to 2019-23	483.376636	281.9764567	0.000
1959-63 to 2009-13	326.358368	281.9764567	0.008313491
1959-63 to 2014-18	493.18516	281.9764567	0.000
1959-63 to 2019-23	445.751456	281.9764567	0.000
1964-68 to 2009-13	369.400212	281.9764567	0.001148723
1964-68 to 2014-18	536.227004	281.9764567	0.000
1964-68 to 2019-23	488.7933	281.9764567	0.000
1969-73 to 2009-13	327.020356	281.9764567	0.008077065
1969-73 to 2014-18	493.847148	281.9764567	0.000
1969-73 to 2019-23	446.413444	281.9764567	0.000

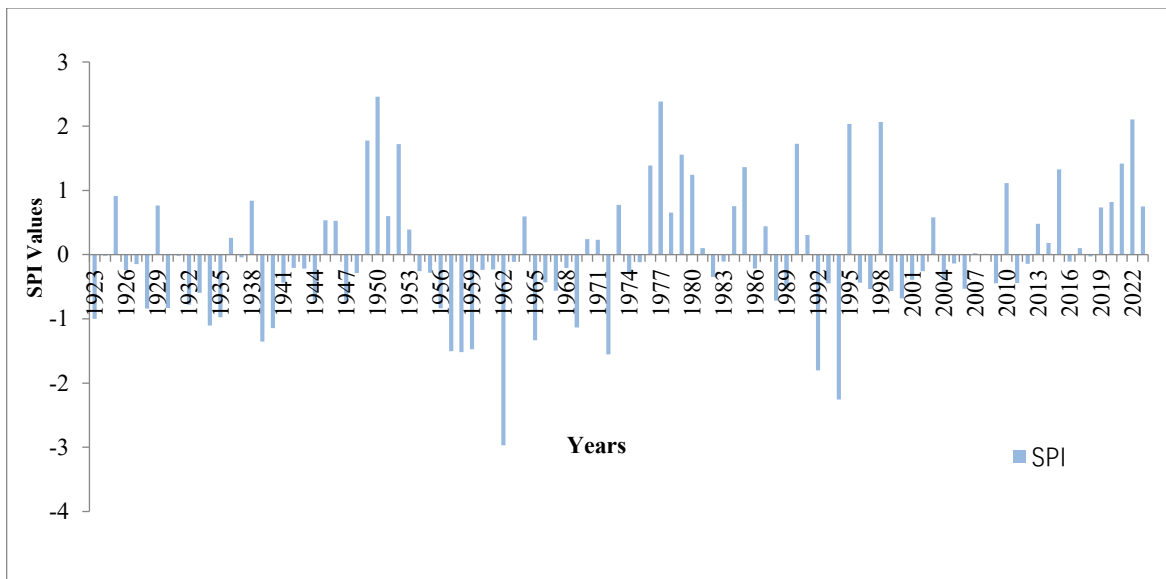
1974-78 to 2014-18	322.464988	281.9764567	0.009839879
1979-83 to 2014-18	382.39774	281.9764567	0.000609359
1979-83 to 2019-23	334.964036	281.9764567	0.005689575
1984-88 to 2014-18	355.92062	281.9764567	0.002180585
1984-88 to 2019-23	308.486916	281.9764567	0.017728112
1994-98 to 2014-18	315.673644	281.9764567	0.013141453
1999-03 to 2014-18	324.767688	281.9764567	0.008908273
2004-08 to 2014-18	287.38238	281.9764567	0.040869872

(Source: Compiled by Authors)

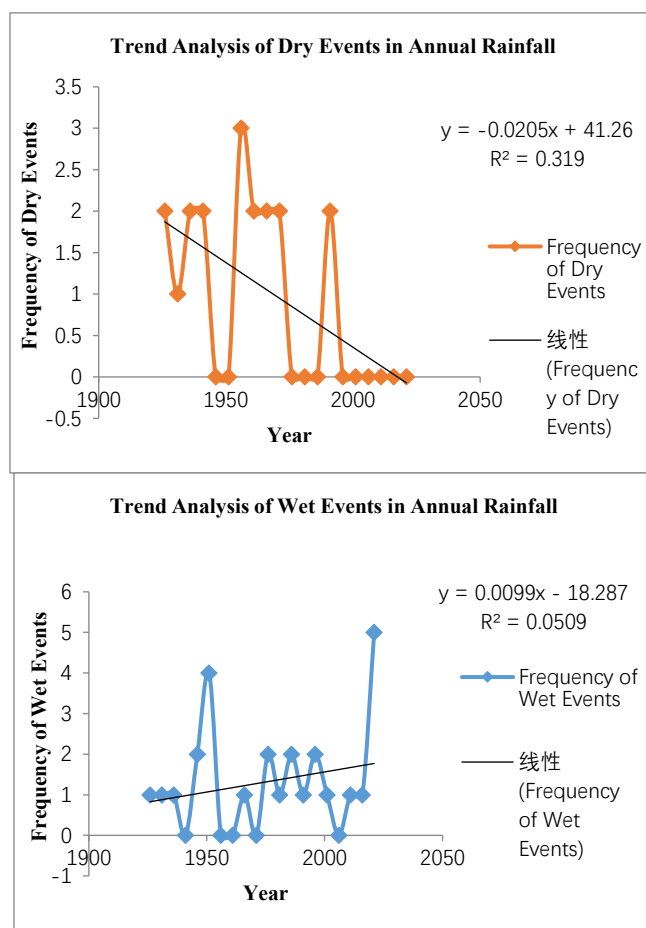
Table 9 shows that the monsoon rainfall has undergone significant variations over the decades, mainly in the post-1950s period. Here, cluster 1949-53 shows the most significant differences. The variability in the monsoon rainfall clusters is more or less gradual over time, indicating steady shifts over decades. The fewer total cluster differences in monsoon rainfall can be associated to the fewer mean differences between clusters. But from Table 8 and Figure 4, it could be noticed that the within-cluster variability is higher, but the coefficient of variation is lower in monsoon rainfall, respectively. This happened because within five years, the fluctuation is high in the monsoon season, but the CV remains lower due to very high mean monsoon rainfall. A similar pattern could be noticed in the case of winter rainfall (Table 10), which also shows significant variations among clusters, mainly in the post-1950s period. The most different cluster in this season is 1989-93. The total number of cluster variability is less in winter rainfall, which illustrates that the mean differences between the clusters are insignificant, as Table 8 signifies that within-cluster variability is higher in winter rainfall. But Figure 4 shows higher CV in winter rainfall. This situation indicates that, as the mean winter rainfall is very low, it increases the coefficient of variation. Unlike the monsoon and winter seasons, significant rainfall variability could be observed in the recent decades in the summer season, where the most varied clusters are 2009-13, 2014-18, and 2019-23 (Table 11). Starting from 1924-28, the previously mentioned clusters significantly differ from almost every half-decadal cluster spanning over a hundred years, which signifies that the current decadal rainfall is majorly varying from the last century decades. Table 8 clarifies that the between-cluster differences are higher than the within cluster differences in summer rainfall. Therefore, the cluster mean differences are higher than the monsoon and winter seasons. Also, from Figure 4, it is observed that the CV is comparatively moderate, which signifies that cluster-to-cluster variability is higher compared to year-to-year fluctuations in summer precipitation.

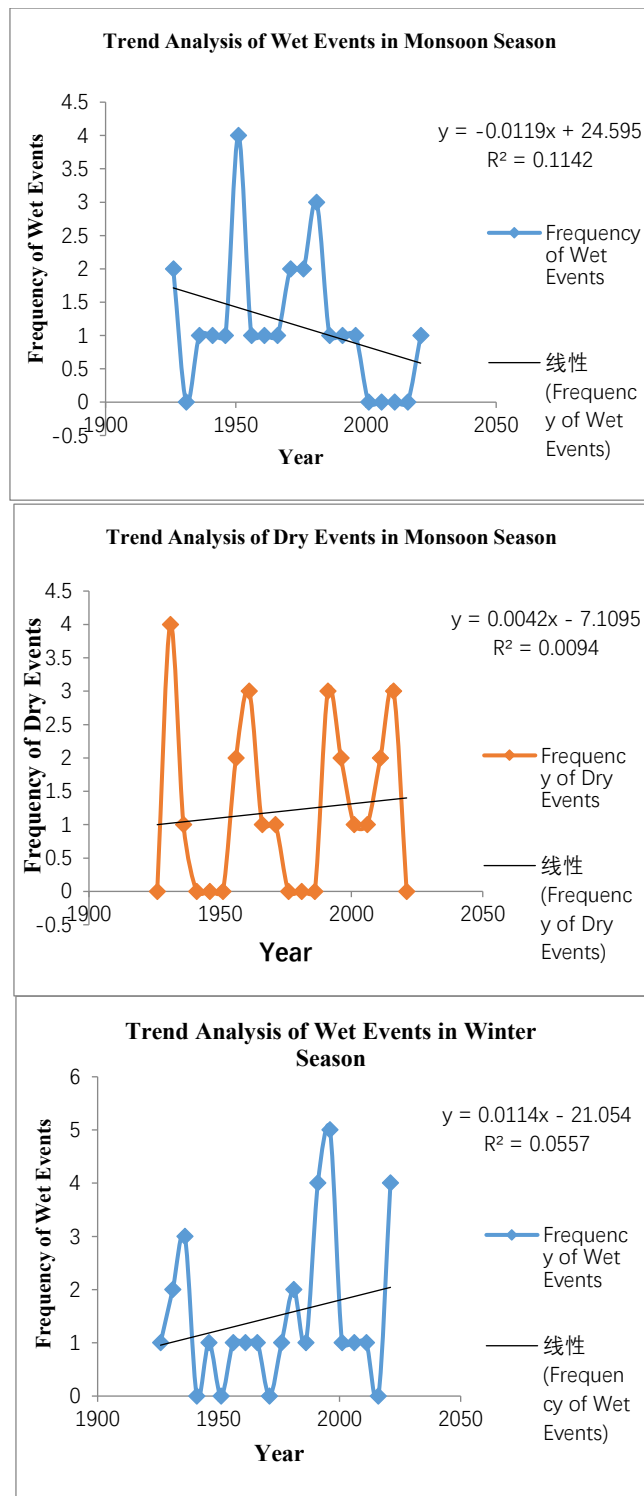
### 3.5. Standardized Precipitation Index

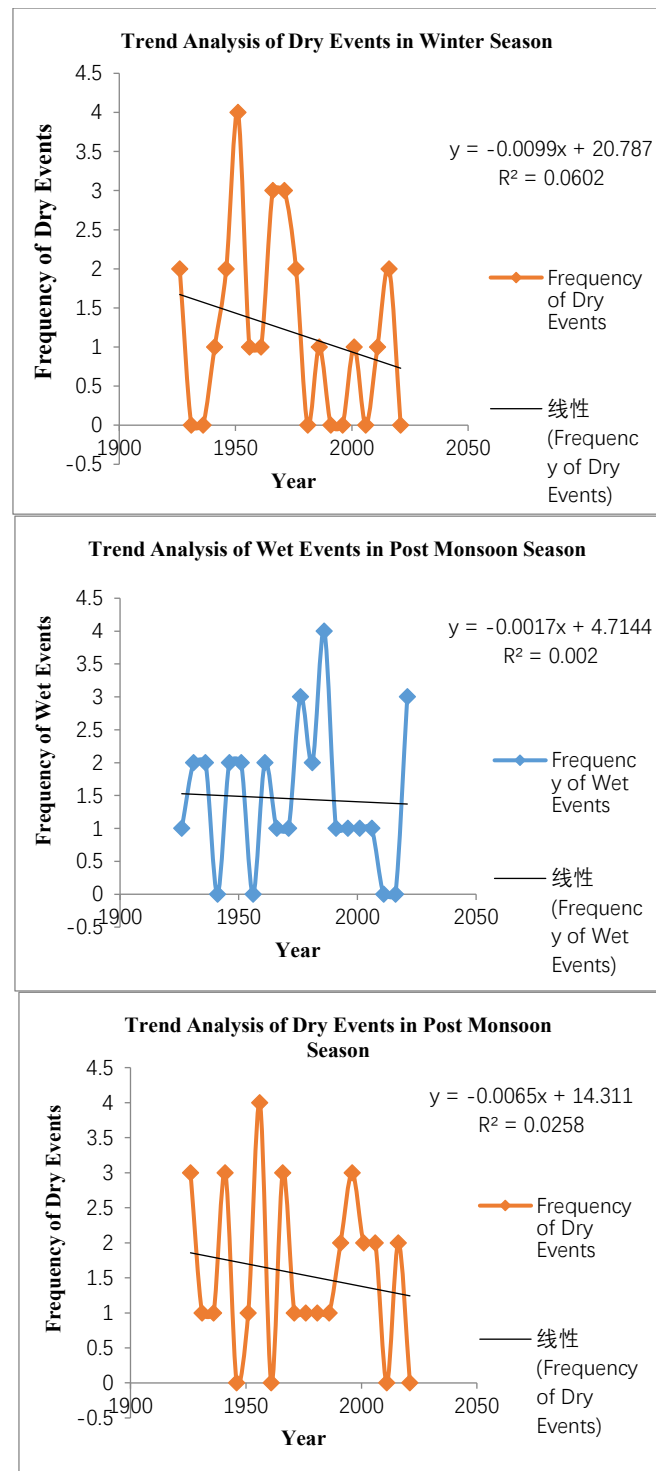
SPI has been computed on annual and seasonal rainfall data to detect the extreme wet and dry events (Figure 5). The majority of the years fall under near normal, however there are several occurrences of wet and dry periods. 1950, 1977, 1995, 1998, and 2022 fall under extreme wet events. Besides, very wet events occurred in 1949, 1952, 1979, and 1990. On the other hand, 1962 and 1994 exhibit extreme dry periods, and 1957, 1958, 1972, and 1992 illustrate the occurrences of very dry events. In the monsoon season, very wet and extreme wet events occurred in the mid-20<sup>th</sup> century, which are 1949, 1951, 1964, 1995, and 1950, 1998, respectively. Besides, very dry and extreme dry events took place in 1959, 1992, 1994, 2001, 2016, and 1962, which started in the mid twentieth century, but extended in recent decades. In the case of the winter season, the years 1997, 2007, and 1990 have been marked as very wet and extremely wet, respectively. On the other hand, the years 1925, 1947, 1948, 1951, and 1971 showed the occurrences of very dry events, and the only year 1967 illustrates the occurrence of an extreme dry event. In the post monsoon season, the years 1925 and 1977 exhibit very wet periods, whereas 1929, 1952, 1968, 1973, and 1979 are marked as extreme wet periods. In the case of dry periods, very dry events occurred in 1950, 1957, 1964, and extreme dry events happened in 1940, 1951, and 1954. The summer season exhibits the highest number of occurrences of wet periods in recent decades. In this case, very wet periods occurred in 1977, 2010, 2013, 2016, 2017, 2018, 2019, and 2023, while extreme wet events occurred in the 2015 and 2022. But the happenings of very dry and extremely dry events are comparatively less in the post monsoon season, which are 1939, 1957, and 1962, respectively.



**Figure 5.** Standardized Precipitation Index for Annual Rainfall (1923-2023).







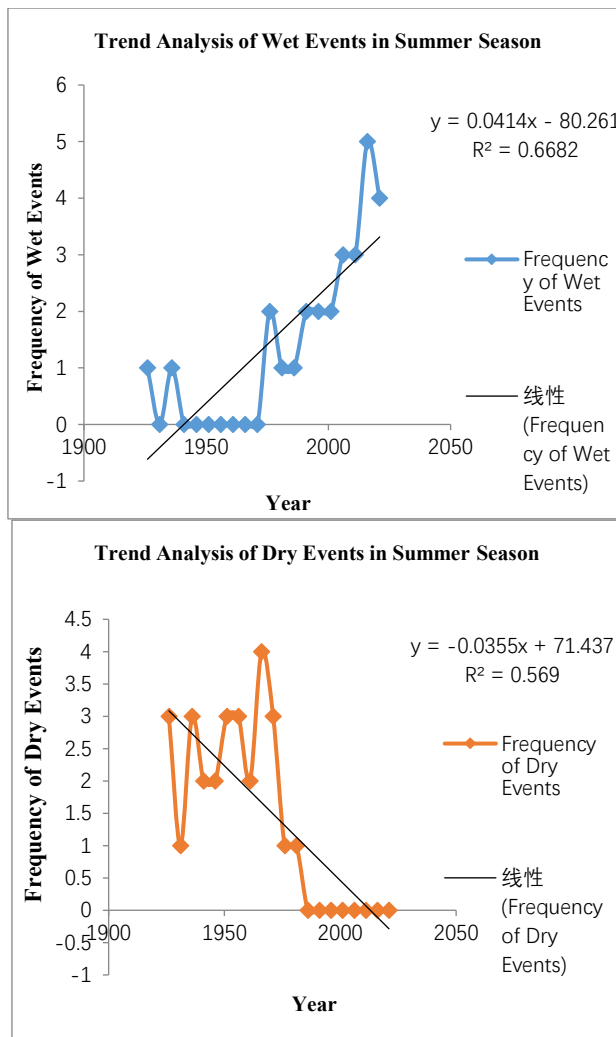


**Figure 6.** Linear Trend Analysis of SPI of Annual and Seasonal Rainfall.

**Table 12.** Linear Regression Results of Wet Events of Annual and Seasonal Rainfall (1923-2023).

Time Period	Coefficient	R	R <sup>2</sup>	P Value	SE	Significance
Annual	0.00992	0.225514869	0.050856956	0.339079	0.010106	No
Monsoon	-0.01087	0.291881886	0.000236407	0.225309	1.321256	No
Winter	0.01157	0.222082535	0.222082535	0.360821	0.01233	No
Post Monsoon	-0.00165	0.04452055	0.001982079	0.49879	0.009367	No
Summer	0.04135	0.817414041	0.668165714	0.000***	0.006869	Yes

Significance Level \* = 0.1, \*\* = 0.05, \*\*\* = 0.01 (Source: Compiled by Authors)

**Table 13.** Linear Regression Results of Dry Events of Annual and Seasonal Rainfall (1923-2023).

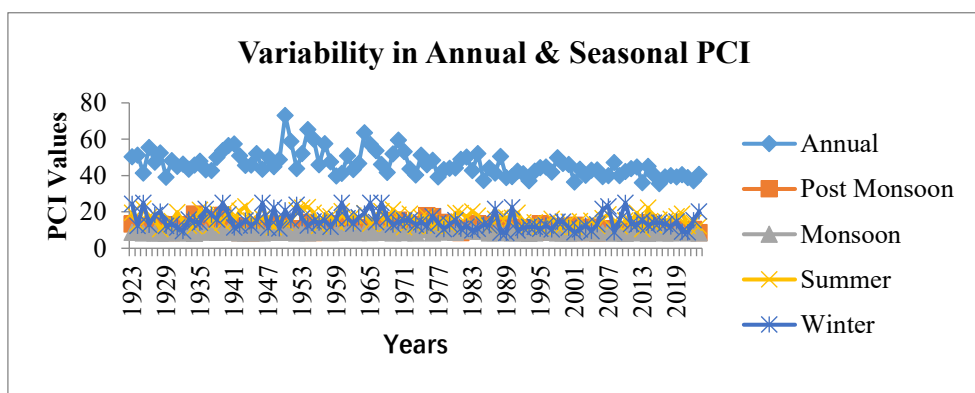
Time Period	Coefficient	R	R <sup>2</sup>	P Value	SE	Significance
Annual	-0.02045	0.56476769	0.31896254	0.0094**	0.00704	Yes
Monsoon	0.00070	0.01537552	0.00023640	0.9501	0.01106	No
Winter	-0.00877	0.20331251	0.04133597	0.4038	0.01024	No
Post Monsoon	-0.00646	0.16060100	0.02579268	0.4987	0.00936	No
Summer	-0.03548	0.75430550	0.56897679	0.000***	0.00728	Yes

Significance Level \* $=0.1$ , \*\* $= 0.05$ , \*\*\* $= 0.01$  (Source: Compiled by Authors)

**Figure 6** shows the trends in extreme wet and dry events. The occurrences of wet events are gradually increasing from 1923 to 2023 for annual, winter, and summer seasonal rainfall patterns and a decrease in wet events for the monsoon season which are visible from the trend analysis (**Figure 6**). For dry periods, the annual, summer, and winter seasons exhibit a declining trend, however, the monsoon is showing a rising trend. Conversely, in the post monsoon season, both the wet and dry events illustrate a declining trend (**Figure 6**). To assess the significance of long-term linear trend, linear regression has been performed for both wet and dry events (**Tables 12 & 13**). From these tables, it is clear that only the summer season is showing a statistically significant increase in wet events. For dry periods, the annual period and summer season indicate a statistically significant reduction in dry event occurrences. It could be attributed to the warming-induced moisture availability, glacier and snowmelt contribution to moisture, and heavy rainfall events, particularly in summer.

### 3.6. Precipitation Concentration Index

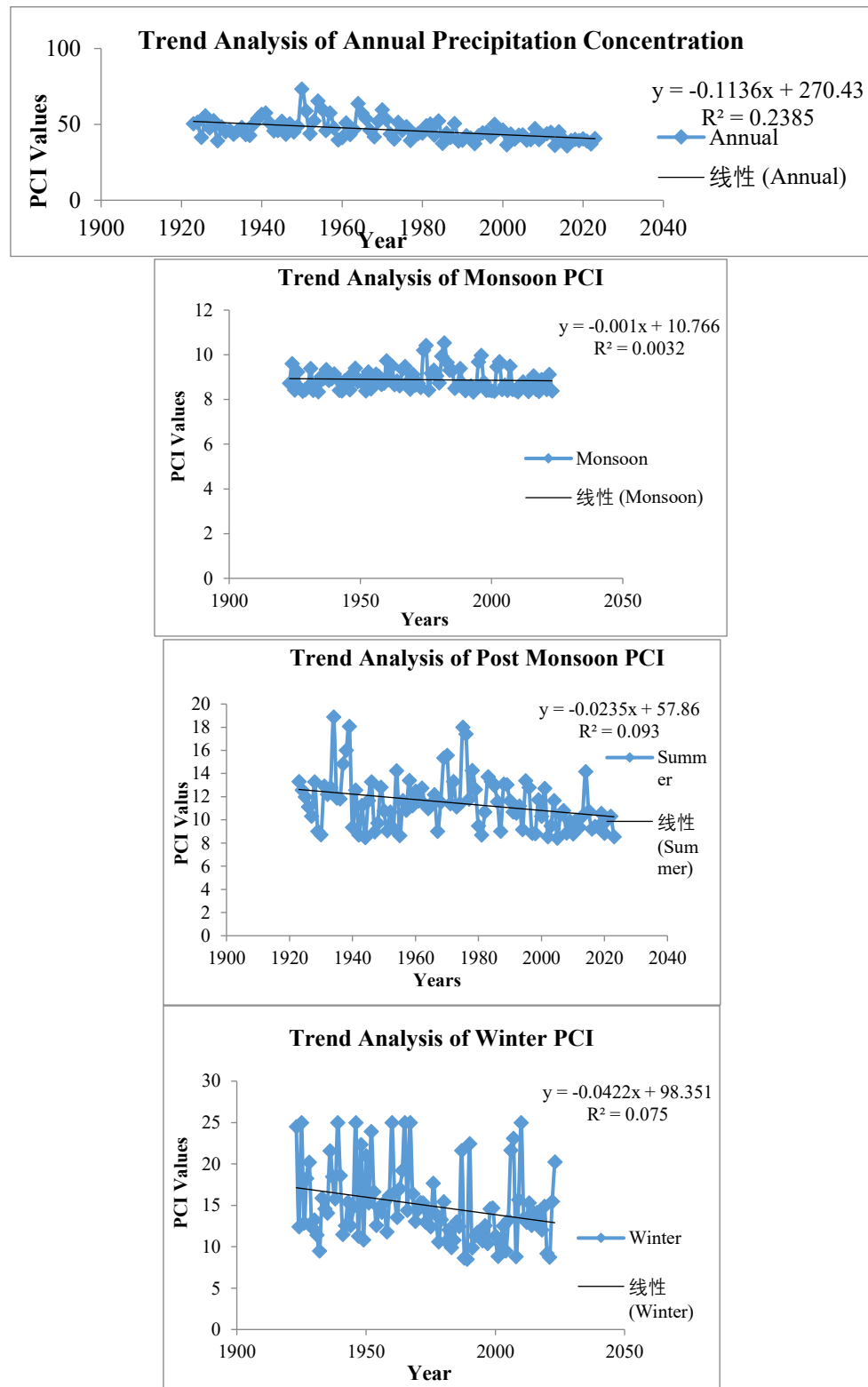
The precipitation concentration index shows the distribution of rainfall across seasons and annual timeline (Figure 7). All of the PCI values of annual rainfall have fallen above 20, which signify strong irregular precipitation distribution over the period or precipitation concentrated in fewer months. Throughout the observation, PCI shows interannual variability where the value of concentration reached 65 in 1954 and 60 in 1955. In contrast, the lowest value of concentration has occurred in 2016 with 35 and 36 points in 2013 and 2001. However, after 1980, the fluctuations appear to be reduced. In seasonal precipitation concentration, most variability could be seen in summer and winter rainfall. Majority of the years under these two seasons have fallen under moderate to irregular precipitation concentration. The highest value of strong irregular concentration in the case of summer and winter rainfall has reached 23 in 1943 and 25 in 1925, 1939, 1946, 1960, 1965, 1967, 2010, besides, the lowest concentration was observed as 10.6 in 1928, 2013, and around 8 in 1988, 1989, 2001, 2008, 2021, respectively. The post monsoon season shows less variability compared to summer and winter, but higher variability than the monsoon season. Majority of the years under this season come under moderate precipitation distribution. In this season, the highest value of 18 occurred in 1934 and the lowest occurred in 1929, 1930, 1942, 1944, 1947, 1955, 1981, 1977, 1997, 1998, 2002, 2005, 2008, 2010, 2020 and 2023. On the other hand most uniform precipitation concentration could be identified in monsoon season with highest value of about 10 in 1974, 1975 and 1982 where most of the years have fallen below 10 of precipitation concentration index (**Figure 7**). The above analysis indicates that total annual precipitation is highly irregular as precipitation is not evenly distributed throughout the seasons. Also the post summer and winter seasons exhibit moderate to irregular distribution within the months. The post monsoon season represents a moderate level of concentration but more uniform precipitation concentration could be seen in monsoon season signifying even rainfall distribution within the months.



**Figure 7.** Precipitation Concentration Index showing variability of rainfall Distribution in Annual and Seasonal rainfall from 1923 to 2023.

**Figure 8** represents the trends in annual and seasonal PCI values. The trend analysis shows that the overall concentration in rainfall distribution within seasons and months is reduced throughout the study period (**Figure 8**). To detect the significance of seasonal PCI trends, linear regression analysis has been performed (**Table 14**). From **Table 14**, it is evident that all of the periods show a statistically significant downward trend except the monsoon season. The reduction in irregular precipitation distribution could be attributed to multiple factors. Increasing rainfall amount, particularly for winter and summer seasons

(Figure 9), contributes to the declining irregularity in rainfall distribution. Similarly, if the total rainy days rise uniformly within months, it may also reduce intra seasonal rainfall concentration. In the context of the post monsoon season, as the trend analysis of yearly average rainfall is not significant, the decline in PCI may be due to the even distribution of rainy days or the long-term balanced distribution of rainfall. Besides, as three seasons show declining PCI over the study period, the annual PCI is also shows a declining trend, reinforcing the evidence of a shift toward a less irregular distribution of rainfall pattern over time.



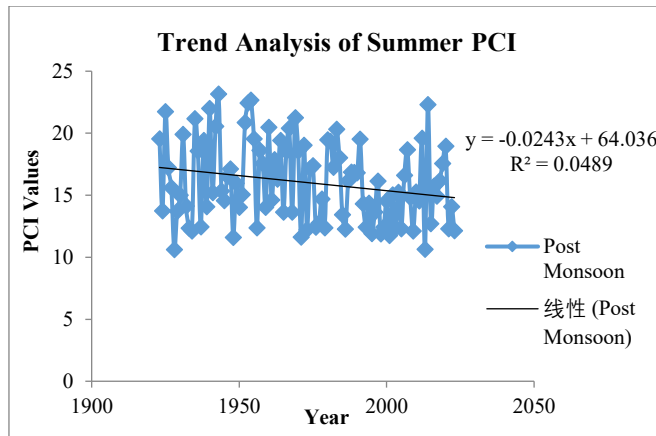


**Figure 8.** Linear Trend Analysis of Annual and Seasonal Precipitation Concentration Index (1923-2023).

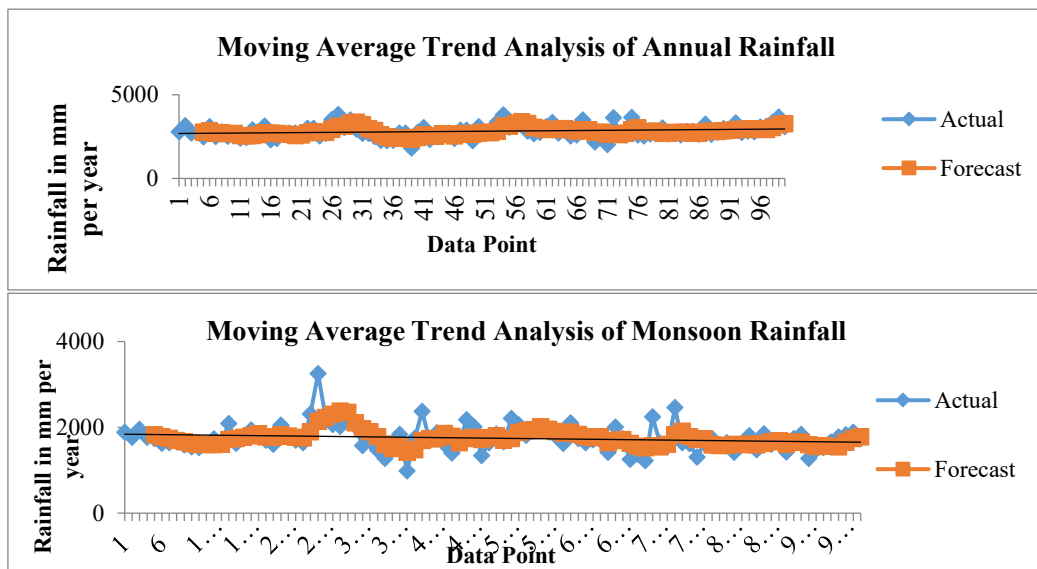
**Table 14.** Linear Regression Results of Annual and Seasonal PCI (1923-2023).

Time Period	Coefficient	R	R2	P Value	SE	Significance
Annual	-0.1136129	0.488343	0.238479	0	0.020405	Yes
Monsoon	-0.0009533	0.056745	0.00322	0.573001	0.001686	No
Post Monsoon	-0.0235233	0.304905	0.092967	0.001933	0.007385	Yes
Winter	-0.0422385	0.273779	0.074955	0.0056	0.014913	Yes
Summer	-0.0243355	0.221224	0.04894	0.026201	0.010782	Yes

Significance Level \* = 0.1, \*\* = 0.05, \*\*\* = 0.01 (Source: Compiled by Authors)

### 3.8. Trend Analysis

The simple moving average method is computed to visualize the yearly and seasonal rainfall trends in Figure 9. The annual rainfall is showing an increasing trend, expanding over a century. Similarly, winter, summer, and post monsoon rainfall also exhibit an upward trend over the years. But in the monsoon season, it illustrates a significant decreasing trend (Figure 9). Further, the regression analysis has been performed to check the significance of the trend analysis at 10%, 5%, and 1% significance intervals (Table 15). This test result indicates that the annual, monsoon, winter, and summer rainfall trends are statistically significant with P values of 0.02, 0.08, 0.02, and 0.00, respectively, but for post monsoon season, it is not statistically significant, where the P value is 0.81.



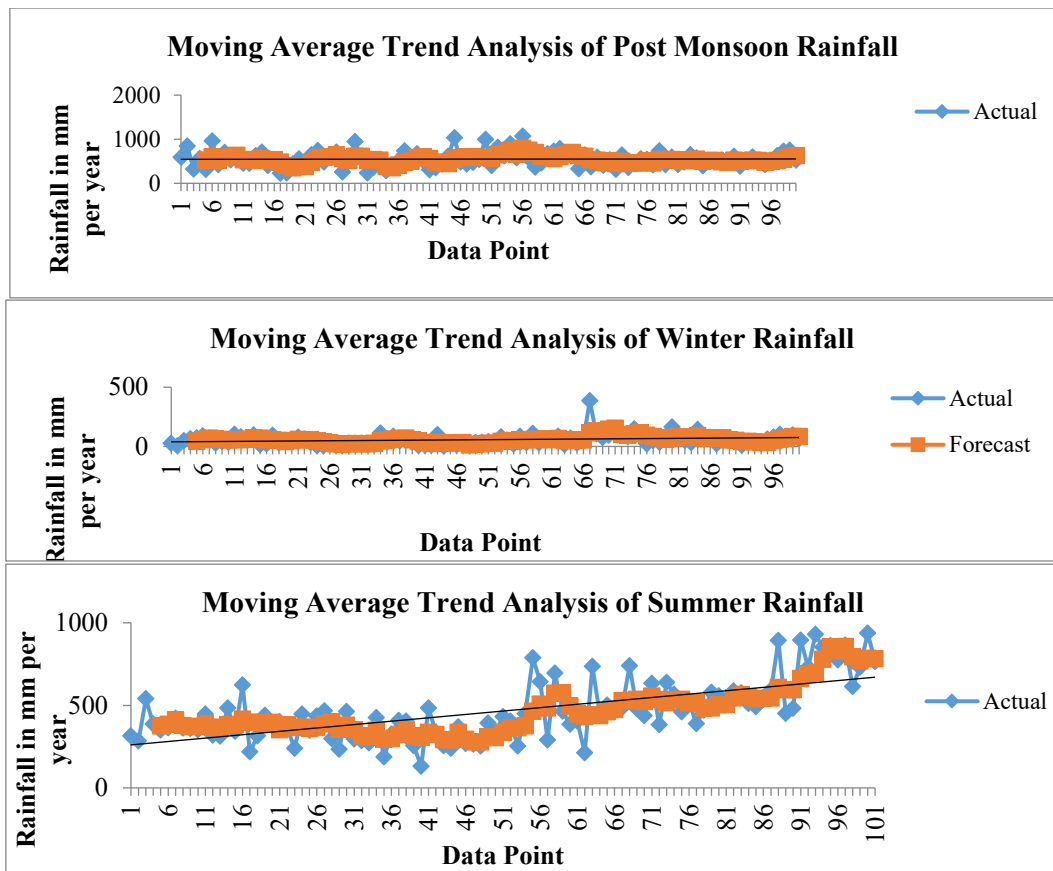
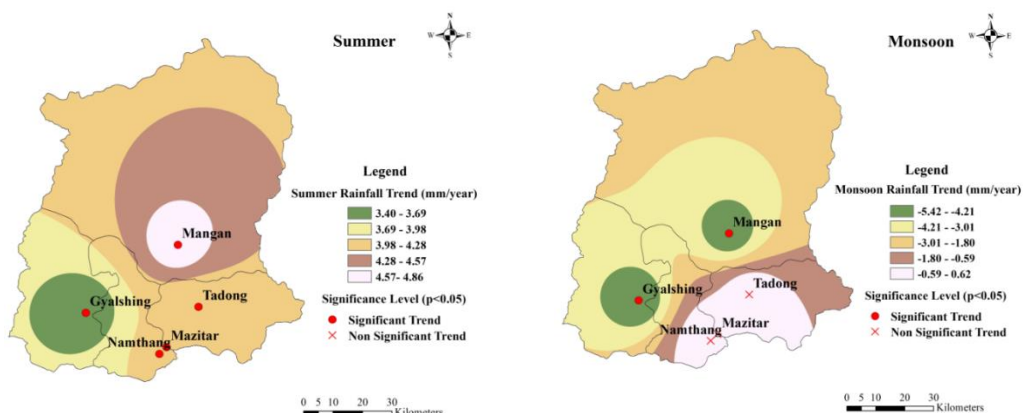


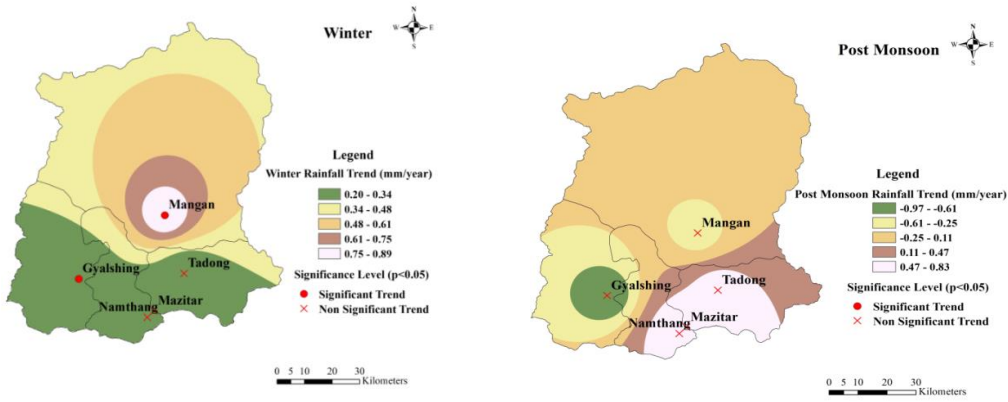
Figure 9. Linear Trend Analysis of Annual and Seasonal Rainfall from 1923-2023.

Table 15. Linear Regression Results of Annual and Seasonal Average Rainfall (1923-2023).

Time Period	Coefficient	R	R2	P Value	SE	Significance
Annual	2.83981243	0.218607	0.047789	0.02807**	1.274013	Yes
Monsoon	-1.7665570	0.171871	0.02954	0.085687*	1.017645	Yes
Post Monsoon	0.14322664	0.024063	0.000579	0.811221	0.598052	No
Winter	0.16037843	0.220683	0.048701	0.026578**	0.160378	Yes
Summer	4.10208712	0.654529	0.428408	0.000***	0.476213	Yes

Significance Level \* $=0.1$ , \*\* $=0.05$ , \*\*\* $=0.01$  (Source: Compiled by Authors)





**Figure 10.** Spatial Trend Analysis of Seasonal Rainfall across Sikkim from 1923-2023 based on IDW Interpolation Technique.

Figure 10 depicts the spatial distribution of seasonal precipitation trends of the five weather stations in Sikkim. The analysis identifies significant and non-significant trends based on a p value less than 0.05. For the summer season, all the stations show a significant increasing trend, where Mangan illustrates the highest positive rainfall trend. From the spatial distribution map, it could be clearly identified that the higher increasing summer rainfall is concentrated in the northeastern part of the state. Conversely, the lowest increasing trend is concentrated around Gyalshing. A notable decreasing trend could be noticed in monsoon rainfall in all the stations. The highest decrease in monsoon rainfall can be found around Mangan and Gyalshing stations. Though the remaining stations also show a notable decline, but these are not statistically significant. A similar pattern is identified in winter rainfall, where Mangan and Gyalshing are exhibiting a significant upward trend. However, in contrast, Namthang, Mazitar, and Tadong are showing a non-significant rising trend. Here, the Mangan also shows the highest positive trend, and the higher concentration of positive winter rainfall is concentrated in the central part of the state. These suggest localized variations in monsoon and winter rainfall trends, with certain regions experiencing more pronounced changes. Besides, both positive and negative rainfall trends can be seen in post monsoon season. The positive precipitation trend is concentrated around Namthang, Mazitar, and Tadong stations in the southeastern part of the state. On the other hand, negative trends could be noticed around Gyalshing and Mangan. However, these trends values are not significant for the post monsoon season. The result highlights spatial heterogeneity in the seasonal rainfall trends, where the northern and southern stations show consistent trends, whereas, the southern and eastern stations are not statistically significant. The significant positive trends in Mangan and Gyalsing during the summer and winter seasons and negative trends in the monsoon season suggest potential climatic shifts in the rainfall distribution in Sikkim.

**Table 16.** Root Mean Square Error Analysis for Seasonal Rainfall Trend of Five Weather Stations.

Station	Summer			Monsoon			Post Monsoon			Winter		
	AV	IV	RMSE	AV	IV	RMS E	AV	IV	RMS E	AV	IV	RMS E
Gyalshing	3.40 07	3.4 00	0.00 14	5.41 8	5.41 8	0.00 099	0.96 88	0.96 88	0.000 073	0.19 90	0.19 90	0.000 055
Mangan	4.86 075	4.8 60	-	5.25 9	5.25 9	-	-	-	-	0.89 22	0.89 20	-
Majitar	4.08 3	4.0 07	-	0.61 5	0.61 5	-	0.71 40	0.71 40	-	0.23 79	0.23 79	-
Namthang	4.08 3	4.0 09	-	0.61 5	0.61 3	-	0.71 40	0.71 40	-	0.23 79	0.23 79	-
Tadong	4.08 3	4.0 82	-	0.61 5	0.61 5	-	0.71 40	0.71 40	-	0.23 79	0.23 79	-

AV= Actual Values, IV= Interpolated Values, RMSE= Root Mean Square Error (Source: Compiled by Authors)

**Table 16** further supports the spatial trend analysis by presenting the accuracy assessment of the IDW trend analysis of seasonal rainfall. Similar to the mean rainfall interpolation (Table 4), the trend analysis exhibits very close actual and interpolated values for all the weather stations and seasons. The root mean square error is 0.0014 for summer, 0.00099 for monsoon, 0.000073 for post monsoon and 0.0005 for winter season. Hence, the interpolated trend results are reliable for all the seasons.

#### 4. Discussion

*Several long-term studies (Kakkar et al., 2022; Sharma et al., 2025; Guhathakurta & Rivadekar, 2017) confirm the declining trend in monsoon rainfall and increasing summer and winter precipitation, broadly consistent with our results, though differences in time frames and datasets explain some discrepancies.* While the findings of some of the previous research align with our study, the present work advances the existing research by incorporating a holistic methodological analysis of rainfall dynamics in Sikkim. The outcomes reveal some new insights such as- short term variation is higher in case of monsoon and winter rainfall but long term variability is more in summer rainfall; the extreme wet events are rising and dry events are declining in summer season; annual rainfall shows higher irregularity but summer, post monsoon and winter rainfall shows moderate to high irregularity while most uniform concentration can be seen in monsoon rainfall. But the irregularity is significantly decreasing in all seasons except monsoon. The trend analysis also exhibits spatial variation. The monsoon rainfall shows a declining trend at all the stations, with the highest in Mangan and Gyalshing. Summer rainfall exhibits an increase in all stations, with the in Gyalshing, followed by Mangan. Winter rainfall also shows an increase in all stations, but significantly around Gyashing. While Post Monsoon shows a statistically insignificant trend for all the stations. This comprehensive approach enables a more in-depth understanding of the variability of climatic shifts in precipitation. These nuanced insights, coupled with spatial mapping, enrich and strengthen the precipitation behavior across the state.

Based on the above insights, it is necessary to identify potential climatic drivers that may explain the seasonal climatic shifts. The summer rainfall is exhibiting a major increasing trend, which is likely linked to the stronger orographic updrafts of moisture-laden wind due to rising temperature; retreating glaciers and snow cover may contribute to increasing surface temperature and providing more moisture which is affecting precipitation pattern. In the case of the winter season, the increasing rainfall may be attributed to the moisture holding capacity due to the warming of winter temperatures in the Himalayas, rising occurrences of western disturbances, which can extend further east due to a shift in the westerly jet stream, increasing post monsoon season cyclonic activities over Indian Ocean, etc. (Bhutiyani et al., 2007; Vellore et al., 2022; Varikoden et al., 2022; Priya et al., 2022). Conversely, the rainfall decreases during the monsoon season may be connected to several factors. The rising temperature of the Indian Ocean is disrupting the land-sea surface temperature contrast, vital for rainfall over the country (Roxy et al., 2014; Preethi et al., 2017). The monsoon rainfall became shorter but more intense, which resulted in a net decrease in total monsoon rainfall. The warming of the Tibetan plateau is causing changes in upper-level wind circulation. This warming increases surface temperature, leading to stronger thermal updrafts. This enhanced vertical motion and adiabatic cooling effect decreases the upper tropospheric temperature over the Tibetan anticyclone region, which is weakening the Tropical Easterly Jet, and in turn may be attributed to weaker monsoon rain (Rao et al., 2022). The increasing frequency of ENSO events is also likely linked to the weaker monsoonal rainfall over the country (Kumar et al., 2007).

The above analysis represents significant rainfall variability in Sikkim, which remarkably influences the livelihood of people. The findings clearly demonstrate a changing and erratic precipitation pattern across the state. The altered precipitation pattern is assumed to be more erratic in the future (Singh & Goyal, 2016). The changing climatic conditions, such as irregular precipitation, are harsh on mountain rural communities of Sikkim, who primarily depend on subsistence agriculture for livelihood (Azhoni & Goyal, 2018). As most farmers depend on rainfall for agriculture, the varied rainfall pattern can affect agricultural productivity in the absence of irrigation facilities. Moreover, the changing rainfall pattern can also have a cascading effect on the water resource availability, groundwater recharge, soil moisture, etc., which are essential for sustaining agricultural practices and drinking water supply. The higher variability in rainfall could affect soil fertility and increase the risks of crop failure. The changing climatic pattern is affecting the pasture lands at every altitude of mountainous terrain, which is severely impacting livestock farming and their productivity (Sharma & Rai, 2012). In addition, a shift in seasonal rainfall patterns could influence the occurrences of extremes weather events, giving rise to flash floods and landslides, further exacerbating the vulnerability of local communities.

#### 5. Conclusion

The study presents a century-long comprehensive assessment of yearly and seasonal precipitation

distribution, variability, and trends in Sikkim. The findings revealed significant fluctuations in precipitation, especially for summer and winter rainfall. The monsoon precipitation is declining over the years while summer and winter rainfall is increasing. The extreme wet and dry events tend to increase in summer seasons. The irregularity in precipitation is also declining in summer and winter season. The increased rainfall variability can challenge traditional farming systems by posing threats to water availability, food security, and raise risks of natural hazards. *Adaptation strategies should focus on climate-resilient agriculture (e.g., drought-tolerant crops, irrigation innovations), sustainable water management (rainwater harvesting, groundwater recharge), livestock resilience (fodder storage, veterinary services), and disaster preparedness (early warning systems, community awareness).* The future works can be oriented towards community-based adaptation strategies, combining indigenous knowledge with a modern scientific approach to strengthen livelihood resilience.

#### Discloser Statement

The authors declared no potential conflicts of interest.

#### Data availability

The link of the processed dataset is given below:

<https://docs.google.com/spreadsheets/d/12YcL7QkdJUSBRJuVBDCXLC-jbJPWmlBM/edit?usp=sharing&ouid=118375851847902707828&rtpof=true&sd=trueFunding>

#### Disclosure

This research received no specific grant from any funding agency.

#### References

Abdi, H. and Williams, L. J., 2010. Tukeys Honestly Significant Difference (HSD) Test. *Encyclopedia of Research Design*, 3(1), pp.1-5.

Abdi, H., 2010. Coefficient of Variation. *Encyclopedia of Research Design*, 1(5), pp.169-171

Agada, I. O., Oguche, C. A. and Agada, P. O., 2018. Analysis of the variability in some climatic parameters in Oyo, Nigeria. *Trends in Science & Technology Journal*, 3(2), pp.401–406.

Agbangba, C.E., Aide, E.S., Honfo, H. and Kakai, R.G., 2024. On the Use of Post-Hoc Tests in Environmental and Biological Sciences: A Critical Review. *Helijon*, 10(3). <https://doi.org/10.1016/j.helijon.2024.e25131>

Azhoni, A. and Goyal, M. K., 2018. Diagnosing climate change impacts and identifying adaptation strategies by involving key stakeholder organisations and farmers in Sikkim, India: Challenges and opportunities. *Science of the Total Environment*, 626, pp.488–477. <https://doi.org/https://doi.org/10.1016/j.scitotenv.2018.01.112>

Basu, R., Misra, G. and Sarkar, D., 2021. A remote sensing based analysis of climate change in Sikkim supported by evidence from the field. *Journal of Mountain Science*, 18(5), pp.1256–1267. <https://doi.org/10.1007/s11629-020-6534-0>

Belay, A., Demissie, T., Recha, J. W., Oludhe, C., Osano, P. M., Olaka, L. A., Solomon, D. and Berhane, Z., 2021. Analysis of climate variability and trends in Southern Ethiopia. *Climate*, 9(6), pp.1–17. <https://doi.org/10.3390/cli9060096>

Bhatta, G. D., Aggarwal, P. K. and Shrivastava, A., 2015. Livelihood diversification and climate change adaptation in Indo-Gangetic plains: implication of rainfall regimes. *Journal of Agriculture and Environment*, 16, pp.77–94. <https://doi.org/10.3126/aej.v16i0.19841>

Bhutiyani, M. R., Vishwas S. K. and Pawar, N. J., 2007. Long-term trends in maximum, minimum and mean annual air temperatures across the Northwestern Himalaya during the twentieth century. *Climate Change*, 85(1), pp.159–177. <https://doi.org/10.1007/s10584-006-9196-1>

Birara, H., Pandey, R. P. and Mishra, S. K., 2018. Trend and variability analysis of rainfall and temperature in the tana basin region, Ethiopia. *Journal of Water and Climate Change*, 9(3), pp.555–569. <https://doi.org/10.2166/wcc.2018.080>

Buckland, F.A. and Ravenscroft, S.P., 1990. A Refinement of ANOVA in Behavioral Analysis. *The Accounting Review*, 65(4), pp.933-945.

Carbonary, A., Scarpa, M. and Plaza, F.I.M., 2025. Environmental Control of Urban Covered Courtyards in Mediterranean Climates - Comparison between different strategies. *Energy Catalyst*, 1(1), pp.22-34. <https://doi.org/10.61552/EC.2025.002>

Chakraborty, S., Pandey, R. P., Chaube, U. C. and Mishra, S. K., 2013. Trend and variability analysis of rainfall series at Seonath River Basin, Chhattisgarh (India). *International Journal of Applied Sciences and Engineering Research*, 2(4), pp.425–434. <https://doi.org/10.6088/ijaser.020400005>

Chang, K. T., 2016. Introduction to Geographic Information System (Eighth). *McGraw-Hill Higher Education*.

Chettri, N., Tsering, K., Shrestha, A. and Sharma, E., 2018. Ecological Vulnerability to Climate Change in the Mountains: A Case Study from the Eastern Himalayas. *Plant Diversity in the Himalaya Hotspot Region*, January.

Cheval, S., 2015. The Standardized Precipitation Index - An Overview. *Romanian Journal of Meteorology*, 12(1-2)

CUCE, P.M., 2025. Evaporative Cooling Technologies : From Past to Present. *Global Decarbonization Journal*,

pp.1-40. <https://doi.org/10.17184/eac.9493>

Gao, C., 2021. Genome engineering for crop improvement and future agriculture. *Cell*, 184(6), pp.1621–1635. <https://doi.org/10.1016/j.cell.2021.01.005>

Gentile, M., Courbin, F. and Meylan, G., 2012. Interpolating Point Spread Function Anisotropy. *Astronomy & Astrophysics manuscript no. psf\_interpolation*, 549. <http://dx.doi.org/10.1051/0004-6361/201219739>

Gerlitz, J. Y., Macchi, M., Brooks, N., Pandey, R., Banerjee, S. and Jha, S. K., 2017. The Multidimensional Livelihood Vulnerability Index—an instrument to measure livelihood vulnerability to change in the Hindu Kush Himalayas. *Climate and Development*, 9(2), pp.124–140. <https://doi.org/10.1080/17565529.2016.1145099>

Getahun, G. W., Zewdu Eshetu, and Mekuria Argaw., 2016. Temporal and spatial variability of rainfall distribution and evapotranspiration across altitudinal gradient in the Bilate River Watershed, Southern Ethiopia. *African Journal of Environmental Science and Technology*, 10(6), pp.167–180. <https://doi.org/10.5897/AJEST2015.2029>

Ghosh, M., and Ghosal, S., 2021. Climate change vulnerability of rural households in flood-prone areas of Himalayan foothills, West Bengal, India. *Environment, Development and Sustainability*, 23(2), pp.2570–2595. <https://doi.org/10.1007/s10668-020-00687-0>

Guhathakurta, P. and Revadekar, J., 2017. Observed Variability and Long-Term Trends of Rainfall Over India. In Observed Climate Variability and Change over the Indian Region. *Ministry of Earth Sciences, Government of India*, pp. 1–16. <https://doi.org/10.1007/978-981-10-2531-0>

Gunawat, A., Sharma, D., Sharma, A. and Dubey, S. K., 2022. Assessment of climate change impact and potential adaptation measures on wheat yield using the DSSAT model in the semi-arid environment. *Natural Hazards*, 111(2), pp.2077–2096. <https://doi.org/10.1007/s11069-021-05130-9>

Hänsel, S., Schucknecht, A. and Matschullat, J., 2016. The Modified Rainfall Anomaly Index (mRAI)—is this an alternative to the Standardised Precipitation Index (SPI) in evaluating future extreme precipitation characteristics? *Theoretical and Applied Climatology*, 123(3–4), pp.827–844. <https://doi.org/10.1007/s00704-015-1389-y>

Hansun, S., 2013. A new approach of moving average method in time series analysis. *2013 International Conference on New Media Studies, CoNMedia 2013*. <https://doi.org/10.1109/connmedia.2013.6708545>

Health Indicators., 2011. *Health & Family Welfare Department, Government of Sikkim*. <https://sikkim.gov.in/DepartmentsMenu/health-family-welfare-department/State Health Profile/demographic-indicators>

IPCC., 2007. Climate Change 2007: Impacts, Adaptation and Vulnerability. Working Group II Contribution to the Fourth Assessment Report of the Intergovernmental Panel on Climate Change. [https://www.ipcc.ch/pdf/assessment-report/ar4/wg2/ar4\\_wg2\\_full\\_report.pdf](https://www.ipcc.ch/pdf/assessment-report/ar4/wg2/ar4_wg2_full_report.pdf)

IPCC., 2023. Sixth Assessment Report (AR6) Synthesis Report: Climate Change 2023. *An Assessment of the Intergovernmental Panel on Climate Change*, 335(7633), pp.1–85. <https://www.ipcc.ch/report/ar6/syr/>

Johnstone F.R., Boyland, J.E., Meadows, M. and Shale, E., 1999. Some Properties of Simple Moving Average when Applied to Forecasting a Time Series. *Journal of Operational Society*, 50, pp.1267-1271.

Kakkar, A., Rai, P. K., Mishra, V. N. and Singh, P., 2022. Decadal trend analysis of rainfall patterns of past 115 years & its impact on Sikkim, India. *Remote Sensing Applications: Society and Environment*, 26. <https://doi.org/10.1016/j.rsase.2022.100738>

Karavitis, C. A., Alexandris, S., Tsesmelis, D. E. and Athanasopoulos, G., 2011. Application of the Standardized Precipitation Index (SPI) in Greece. *Water (Switzerland)*, 3(3), pp.787–805. <https://doi.org/10.3390/w3030787>

Kumar, M. N., Murthy, C. S., Sesha Sai, M. V. R. and Roy, P. S., 2009. On the use of Standardized Precipitation Index (SPI) for drought intensity assessment. *Meteorological Applications*, 16(3), pp.381–389. <https://doi.org/10.1002/met.136>

Kumar, P., Rupa Kumar, K., Rajeevan, M. and Sahai, A. K., 2007. On the recent strengthening of the relationship between ENSO and northeast monsoon rainfall over South Asia. *Climate Dynamics*, 28(6), pp.649–660. <https://doi.org/10.1007/s00382-006-0210-0>

Kumar, P., Sharma, M. C., Saini, R. and Singh, G. K., 2020. Climatic variability at Gangtok and Tadong weather observatories in Sikkim, India, during 1961–2017. *Scientific Reports*, 10(1), pp.1–12. <https://doi.org/10.1038/s41598-020-71163-y>

Lama, M. P. (2001). *Sikkim Human Development Report*.

Larson, M. G., 2008. Analysis of variance. *Circulation*, 117(1), pp.115–121. <https://doi.org/10.1161/CIRCULATIONAHA.107.654335>

Lee, S. G., Kim, S. K., Lee, H. J., Choi, C. S. and Park, S. T., 2016. Impacts of climate change on the growth, morphological and physiological responses, and yield of Kimchi cabbage leaves. *Horticulture Environment and Biotechnology*, 57(5), pp.470–477. <https://doi.org/10.1007/s13580-016-1163-9>

Li, J. and Heap, A. D., 2011. *A review of spatial interpolation methods for environmental scientists* (Record 2011/23). *Geoscience Australia*. [https://d28rz98at9flks.cloudfront.net/73708/Rec2011\\_023.pdf](https://d28rz98at9flks.cloudfront.net/73708/Rec2011_023.pdf)

Livada, I. and Assimakopoulos, V. D., 2007. Spatial and temporal analysis of drought in Greece using the Standardized Precipitation Index (SPI). *Theoretical and Applied Climatology*, 89(3–4), pp.143–153. <https://doi.org/10.1007/s00704-005-0227-z>

Livers, J.J., 1942. Some Limitations to Use Coefficient of Variation. *Journal of Farm Economics*, 24 (4), pp.892–895.

Macchi, M., Gurung, A. M. and Hoermann, B., 2015. Community perceptions and responses to climate variability

and change in the Himalayas. *Climate and Development*, 7(5), pp.414–425. <https://doi.org/10.1080/17565529.2014.966046>

Michaels, P. J., Balling, R. C., Vose, R. S. and Knappenberger, P. C., 1998. Analysis of trends in the variability of daily and monthly historical temperature measurements. *Climate Research*, 10(1), pp.27–33. <https://doi.org/10.3354/cr010027>

Mishra, P. K., Rai, A. and Rai, S. C., 2020. Land use and land cover change detection using geospatial techniques in the Sikkim Himalaya, India. *Egyptian Journal of Remote Sensing and Space Science*, 23(2), pp.133–143. <https://doi.org/10.1016/j.ejrs.2019.02.001>

Oakes, T., 2009. Asia. *International Encyclopedia of Human Geography*, 1(12). <https://doi.org/10.1016/B978-008044910-4.00250-9>

Ojo, O. I. and Ilunga, M. F., 2017. The Rainfall Factor of Climate Change Effects on the Agricultural Environment: A Review. *American Journal of Applied Sciences*, 14(10), pp.930–937. <https://doi.org/10.3844/ajassp.2017.930.937>

Oliver, J. E. (1980). Monthly precipitation distribution: A comparative index. *Professional Geographer*, 32(3), pp.300–309. <https://doi.org/10.1111/j.0033-0124.1980.00300.x>

Preethi, B., Mujumdar, M., Kripalani, R. H., Prabhu, A. and Krishnan, R., 2017. Recent trends and tele-connections among South and East Asian summer monsoons in a warming environment. *Climate Dynamics*, 48(7–8), pp.2489–2505. <https://doi.org/10.1007/s00382-016-3218-0>

Priya, P., Singh, B.B. and Bisht, J., 2022. Extreme Storms. Assessment of Climate Change over Indian Region. *Ministry of Earth Science, Government of India*, pp. 155–174. <https://doi.org/https://doi.org/10.1007/978-981-15-4327-2>

Rao, K.K., Priya, P., Gandhi, N., Bhaskar, P., Buri, V.K. and Sabade, S. S., 2022. Precipitation Changes in India. Assessment of Climate Change over Indian Region. *Ministry of Earth Science, Government of India*, pp. 47–72. <https://doi.org/https://doi.org/10.1007/978-981-15-4327-2>

Raziei, T., 2021. Revisiting the Rainfall Anomaly Index to serve as a Simplified Standardized Precipitation Index. *Journal of Hydrology*, 602, p.126761. <https://doi.org/10.1016/j.jhydrol.2021.126761>

Roxy, M. K., Ritika, K., Terray, P. and Masson, S., 2014. The curious case of Indian Ocean warming. *Journal of Climate*, 27(22), pp.8501–8509. <https://doi.org/10.1175/JCLI-D-14-00471.1>

Sawyer, S. F., 2009. Analysis of Variance: The Fundamental Concepts. *Journal of Manual & Manipulative Therapy*, 17(2), pp.27–38. <https://doi.org/10.1179/jmrt.2009.17.2.276>

Schröder, L. S., Bhalerao, A. K., Kabir, K. H., Scheffran, J. and Schneider, U. A., 2024. Managing uphill cultivation under climate change – An assessment of adaptation decisions among tribal farmers in Nagaland state of India. *Journal of Environmental Management*, 349, p.119473. <https://doi.org/10.1016/j.jenvman.2023.119473>

Sharma, R. K. and Shreshtha, D. G., 2016. Climate perceptions of local communities validated through scientific signals in Sikkim Himalaya, India. *Environmental Monitoring and Assessment*, 188(578), pp.1–11. <https://doi.org/10.1007/s10661-016-5582-y>

Sharma, G. and Rai, L. K., 2012. Climate Change and Sustainability of Agrodiversity in Traditional Farming of the Sikkim Himalaya. *Climate Change in Sikkim Patterns Impacts, and Initiatives*, 1, pp.193–218.

Sharma, S., Suwa, R., Ray, R. and Mandal, M. S. H., 2022. Correction: Successive Cyclones Attacked the World's Largest Mangrove Forest Located in the Bay of Bengal under Pandemic. *Sustainability*, 14(9), p.5130. <https://doi.org/10.3390/su14159176>

Sharma, K., Chetiya, M. and Baruah, U. D., 2025. 123 Years of Rainfall Trends and Distribution in Gangtok and Itanagar of North East India. *Ecology, Environment and Conservations*, 31(2), pp.679–688. <http://doi.org/10.53550/EEC.2025.v31i02.044>

Sienz, F., Bothe, O. and Fraedrich, K., 2012. Monitoring and quantifying future climate projections of dryness and wetness extremes: SPI bias. *Hydrology and Earth System Sciences*, 16(6), pp.2143–2157. <https://doi.org/10.5194/hess-16-2143-2012>

Sikkim Action Plan on Climate Change., 2011. *Government of Sikkim*, 167.

Sikkim Statistics., 2013. *Government of Sikkim*. <https://sikkim.gov.in/KnowSikkim/statistics/sikkim-statistics>

Singh, V. and Goyal, M. K., 2016. Analysis and trends of precipitation lapse rate and extreme indices over north Sikkim eastern Himalayas under CMIP5ESM-2M RCPs experiments. *Atmospheric Research*, 167, pp.34–60. <https://doi.org/10.1016/j.atmosres.2015.07.005>

State of Forest Report., 2019. Sikkim Forest Statistics. *Indian State of Forest Report- Forest Survey of India*. <http://www.sikkimforest.gov.in/forest.htm>

Tapia-Brito, E. and Riffat, S., 2025. Design and performance analysis of a MopFan-based multi stage air purification system for indoor pollution control. *Green Technology & Innovation*. <https://dx.doi.org/10.36922/gti.7100>

Umar, D. A., Ramli, M. F., Aris, A. Z., Jamil, N. R. and Aderemi, A. A., 2019. Evidence of climate variability from rainfall and temperature fluctuations in semi-arid region of the tropics. *Atmospheric Research*, 224, pp.52–64. <https://doi.org/10.1016/j.atmosres.2019.03.023>

Upadhyay, A., Nigam, N. K., Mishra, P. K. and Rai, S. C., 2024. Climatic variability and its impact on the indigenous agricultural system using panel data analysis in the Sikkim Himalaya, India. *Environmental Monitoring and Assessment*, 196(1). <https://doi.org/10.1007/s10661-023-12193-7>

Upadhyay, A. and Rai, S. C., 2023. Climate Change Analysis in Rangit Basin of Sikkim Himalaya. *Oriental Anthropologist*, 23(1), pp.103–130. <https://doi.org/10.1177/0972558X221147205>

Varikoden, H., Vishnu, S., Koteswararao, K. and Ramarao, M. V. S., 2022. Synoptic Scale Systems. Assessment of Climate Change over Indian Region. *Ministry of Earth Science, Government of India*, pp. 143–154.

<https://doi.org/10.1007/978-981-15-4327-2>

Vellore, R., Priya, P., Boregaonkar, H.P. and Singh, B. B., 2022. Climate Change over the Himalayas. Assessment of Climate Change over Indian Region. *Ministry of Earth Science, Government of India*, pp. 207–222. <https://doi.org/10.1007/978-981-15-4327-2>

Wilks, D. S., 2011. *Statistical Methods in the Atmospheric Sciences* (3rd ed.). Academic Press.

Xu, J., Grumbine, R. E., Shrestha, A., Eriksson, M., Yang, X., Wang, Y. and Wilkes, A., 2009. The melting Himalayas: Cascading effects of climate change on water, biodiversity, and livelihoods. *Conservation Biology*, 23(3), pp.520–530. <https://doi.org/10.1111/j.1523-1739.2009.01237.x>